2-1-2022

# Utah Wintertime Measurements of Heavy-Duty Vehicle Nitrogen Oxide Emission Factors

Gary A. Bishop
*University of Denver*, gabishop10@yahoo.com

Molly J. Haugen
*University of Cambridge*, mollyhaugen@gmail.com

Brian C. McDonald
*Chemical Sciences Laboratory NOAA*

Adam M. Boies
*University of Cambridge*



## Recommended Citation

Bishop, G. A.; Haugen, M. J.; McDonald, B. C.; Boies, A. M., Utah Wintertime Measurements of Heavy-Duty Vehicle Nitrogen Oxide Emission Factors. Environ. Sci. Technol. 2022, 56, (3), 1885-1893, DOI: 10.1021/acs.est.1c06428.

## Publication Statement

This is an accepted manuscript for

Bishop, G. A.; Haugen, M. J.; McDonald, B. C.; Boies, A. M., Utah Wintertime Measurements of Heavy-Duty Vehicle Nitrogen Oxide Emission Factors. Environ. Sci. Technol. 2022, 56, (3), 1885-1893, DOI: 10.1021/acs.est.1c06428.

Copyright held by the American Chemical Society. User is responsible for all copyright compliance.

# Utah Wintertime Measurements of Heavy-duty Vehicle Nitrogen Oxide Emission Factors

*Gary A. Bishop*,†, Molly J. Haugen‡, Brian C. McDonald§ and Adam M. Boies‡*

†Department of Chemistry and Biochemistry, University of Denver, Denver, Colorado 80208, United States of America

‡Department of Engineering, University of Cambridge, Cambridge, United Kingdom CB2 1PZ

§Chemical Sciences Laboratory, National Oceanic and Atmospheric Administration, Boulder, Colorado 80305, United States of America

KEYWORDS

Heavy-duty $NO_x$ emissions, $NO_x$ emission factors, in-use measurements, winter measurements, remote vehicle exhaust sensing

ABSTRACT

There have only been a few wintertime studies of heavy-duty vehicle (HDV) $NO_x$ emissions in the U.S., and while they have observed increased emissions, fleet characterization to identify the cause has been lacking. We have collected wintertime measurements of $NO_x$ emission factors from 1,591 HDV at a Utah Port of Entry in December 2020 that includes individual vehicle identification. In general, the $NO_x$ emission factors for 2011 & newer chassis model year HDV are significantly higher than 2017 spring measurements from California. The newest chassis model year HDV

(2017 - 2021) $NO_x$ emission factors are similar indicating no significant emissions deterioration over the five year period though they are still approximately a factor of 3 higher than the Portable Emissions Measurement on-road enforcement standard. We estimate that ambient temperature increases $NO_x$ emissions no more than 25% in these newer HDV likely through reductions in catalyst efficiencies. $NO_x$ emissions rise to a significantly higher level for the 2011 - 2013 chassis model year vehicles, where within the uncertainties they have emissions similar to older pre-control vehicles indicating they have lost their $NO_x$ control capabilities within eight years. MOVES3 modeling of the Utah fleet under predicted mean $NO_x$ emissions by a factor of 1.8 but the MOVES3 estimate is helped by including a larger fraction of high emitting Glider Kit trucks (new chassis with pre-emission control engines) than found in the observations.

## SYNOPSIS

Wintertime oxides of nitrogen emissions from heavy-duty vehicles are significantly higher than previous warm weather measurements and model estimates.

## INTRODUCTION

In the United States, as in many countries around the world, the movement of freight is often by truck. In 2019 in the U.S. it was estimated that trucking moved more than 70% of the countries freight.[1] The overwhelming majority of these trucks are diesel powered and the resulting nitrogen oxides ($NO_x = NO + NO_2$) and particulate matter (PM) they emit can contribute to air quality problems and produce negative health effects.[2-4] Despite heavy-duty vehicles (HDV) numerically comprising only a small percentage of the on-road fleet (typically around 3 to 4%) nationally they are now estimated to be the largest source of $NO_x$ emissions.[5] $NO_x$ emissions are important precursor emissions not just for ozone but for fine particulates as well. This has led Federal and

California regulators adoption of stringent emission control measures to significantly lower HDV $NO_x$ and PM emissions.

Reductions in $NO_x$ emissions have been sought through the addition of Selective Catalytic Reduction after-treatment systems (SCRs) in 2011 and newer chassis model year HDV.[6] SCRs thermalize an aqueous urea solution to generate ammonia ($NH_3$), which with the help of a catalyst reduces NO and $NO_2$ to nitrogen and water.[7-9] SCRs are however, temperature dependent and the majority of systems in-use (copper zeolite) have a very steep $NO_x$ conversion efficiency curve that starts around a 10% conversion efficiency at 150°C and approaches 90% conversion efficiency above 200°C (Figure S1).[10] Early on in their adoption researchers reported in-use $NO_x$ emissions significantly higher than certification standards when catalyst temperatures are not optimal due to low loads or slow driving speeds.[11-13] As a consequence, the full benefit of in-use $NO_x$ emission reductions have not yet been fully realized.

California's desire to rapidly reduce PM and $NO_x$ emissions from its HDV fleet spawned regulations that went beyond Federal rules with the end result of forcing the retirement of older higher emitting models.[14, 15] Today the California HDV fleet is no longer representative of HDV fleets across the rest of the U.S. with a significantly younger and lower emitting fleet.[8] Since HDV generally have long operating lifetimes (30 or more years) it is unlikely that the retired vehicles were scrapped and more likely they just moved out of state. Because much of the HDV emission research over the past fifteen years has been conducted in California, this has created a large uncertainty in the emissions and fleet characteristics of HDV operating in other states.[5]

Because SCR temperature is an important factor in regulating $NO_x$ emissions in HDV the question of how winter operating conditions affect performance is an important one. Data collected in 2013 and 2014 from the Fort Pitt Tunnel on I-376 in Pennsylvania found higher wintertime $NO_x$

emissions from both light and HDV, however, the difficulty in defining the diesel contribution in a mixed fleet led to large uncertainties in the diesel $NO_x$ emission factors.[16] Summer and winter measurements in 2015 at the Fort McHenry tunnel in Baltimore, MD also showed higher wintertime $NO_x$ emissions for light and HDV.[17] Two newer near-road studies along interstate highways showed stronger links between increased $NO_x$ emissions with decreasing temperatures from HDV.[18, 19] However, all these studies lacked the detailed HDV fleet characterization necessary to eliminate any fleet age changes that may have occurred during the seasonal comparisons that could also explain the differences observed. Research from Europe has shown a $NO_x$ temperature dependence for light-duty diesel vehicles with increasing emissions at lower temperatures, even for vehicles with the newest after-treatment systems, but it's unclear how this might translate to the HDV fleet.[20]

There is supporting evidence that wintertime $NO_x$ inventories may be under reported from recent research showing that winter $PM_{2.5}$ concentrations maxima have not been reduced to the same degree as the summertime maxima.[21] However, there have been conflicting results when evaluating the US National Emissions Inventory (NEI) 2011 and 2014 with atmospheric observations between winter and summer. Summertime studies suggested mobile source $NO_x$ emissions were high by at least 30% relative to atmospheric observations collected.[22-25] By contrast, wintertime aircraft observations of $NO_x$ emissions reported consistency between the NEI 2011 and 2014 with atmospheric observations.[26, 27] While there could be a variety of reasons that contribute to seasonal differences in model-observation comparisons, one possibility is that there are seasonal differences in mobile source $NO_x$ emissions that are not fully accounted for in vehicle emission models. For on-road gasoline engines, the differences in cold-start effects between winter and summer is small for $NO_x$ compared to carbon monoxide (CO) and volatile organic compounds (VOC).[28]

Due to the lack of measurements it is not clear what the impact on $NO_x$ emissions are from heavy-duty diesel engines equipped with SCRs under winter operating temperatures. The cold weather performance of modern HDV fleets is particularly relevant for the Salt Lake City, UT region in the U.S. The mountainous topography in this region is conducive to accumulating fine particulates during periods of low winds and thermal inversions that can be common during the winter months. As a consequence, the region has a serious designation for violation of the 2006 24-hour $PM_{2.5}$ standard.[29] During cold-pool air pollution episodes, the dominant fraction of $PM_{1.0}$ is composed of nitrate ($NO_3^-$) and ammonium ($NH_4^+$). In 2017 the Utah Winter Fine Particulate Study found that when taken together these two species accounted for nearly 80% of the $PM_{1.0}$.[30] With HDV in the Salt Lake City area estimated to be responsible for 45% of the total on-road mobile source $NO_x$ emissions they are an important source to study. This paper reports on wintertime emission measurements collected in Utah from an in-use HDV fleet where the range of emissions technology is large (mechanically controlled engines with no after-treatment systems to SCR equipped electronically controlled engines) that is supported by individual vehicle identification to explore the effects that winter operating conditions have on $NO_x$ emission factors.

## MATERIALS AND METHODS

The Fuel Efficiency Automobile Test (FEAT) is an across-the-road spectroscopic remote exhaust sensor developed at the University of Denver for the unobstructed measurement of pollutants in motor vehicle exhaust, and has been well documented in the literature.[31-34] The instrument has a non-dispersive infrared (IR) component for detecting CO, $CO_2$, hydrocarbons (HC), and percent opacity, and dual dispersive ultraviolet (UV) spectrometers for measuring NO

(205 - 226 nm), $NO_2$ (429 - 446 nm), and $NH_3$ (200 - 215 nm). Collinear beams of IR (carbide ignitor) and UV light (xenon arc lamp) are passed across the roadway into the IR detection unit, and are then focused onto a dichroic beam splitter, which separates the beams into their IR and UV components. The IR light is then passed onto a spinning polygon mirror, which spreads the light across the four infrared detectors: CO (3.6 μm), $CO_2$ (4.3 μm), HC (3.3 μm), and reference (3.9 μm) (opacity is determined from plotting the ratio of the reference vs. $CO_2$ signals). The UV light is reflected off the surface of the beam splitter and focused onto the end of a quartz fiber-optic cable, which transmits the light to dual UV spectrometers.

The exhaust plume path length and optical density of the observed plume are highly variable from vehicle to vehicle, and are dependent upon, among other things, the location of the vehicle's exhaust pipe, wind, and turbulence behind the vehicle. For these reasons, the remote sensor only measures molar ratios of CO, HC, NO, $NO_2$ and $NH_3$ to $CO_2$. These molar ratios are converted into grams of pollutant per kilogram of fuel via carbon mass balance using a carbon mass fraction of 0.86 for diesel fuel and 0.75 for natural gas.[35]

The FEAT detectors were calibrated, as external conditions warranted, from certified gas cylinders containing known ratios of the species to be measured. Because of the reactivity of $NO_2$ with NO and $NH_3$ with $CO_2$, three separate calibration cylinders are needed to cover all of the species: 1) 6% CO, 6% $CO_2$, 0.6% propane, 0.3% NO, nitrogen ($N_2$) balance; 2) 0.05% $NO_2$, 15% $CO_2$, air balance (Praxair); 3) 0.1% $NH_3$, 0.6% propane, balance $N_2$ (Airgas). The measured vehicle molar ratios are normalized to the averaged results of these calibrations to adjust for any variations in the instruments sensitivity and in particular changes in the background $CO_2$ absorption in the optical path.

The FEAT remote sensor is accompanied by a video system that records a freeze-frame image of the license plate of the front of each HDV measured. The images are stored digitally and manually transcribed to incorporate the license plate and state/country into the emissions database. A device to measure the speed and acceleration of vehicles driving past the remote sensor was also used and consists of a pair of infrared emitters and detectors (Banner Industries) which generate a pair of parallel infrared beams passing across the road, 1.83 m apart and approximately 1.5 m above the road. Vehicle speed is calculated from the average of two times collected when the front of the tractors cab blocks the first and the second beam and the rear of the cab unblocks each beam. From these two speeds, and the time difference between the two speed measurements, acceleration is calculated, and reported in mph/s. Outside air temperature was recorded at the site at 5 minute intervals with the use of an Elitech model RC-5+ recording thermometer.

Sampling was conducted at the Utah Department of Transportation Port of Entry located near Perry, UT (~100 km north of Salt Lake City, UT, elev. 1300m) on the southbound lanes of I-15 with measurements collected for approximately 32 hours from Sunday, December 6, to Friday, December 11, 2020 generally between the hours of 8:00 and 19:00 on the exit lane reentering southbound I-15 (Figure S2). The station has two lanes that trucks exiting the interstate are directed into. The west lane has the scales and a posted speed limit of 3 mph while the east lane has a posted speed limit of 20 mph (Figure S3). It is approximately 500 m from the initial highway exit point to the scales and an additional 250 m from the scales to our measurement location with approximately 200 m subject to the speed limits. After the lanes merge the trucks are allowed to accelerate to highway speeds for their return to the freeway. At an average speed of 10 mph (16 kph) a truck will spend less than 5 minutes transiting the station.

The majority of HDV traveling by the site are not required to enter the Port and some companies pay a fee to avoid having to stop at the station. This does not completely exclude these vehicles as any anomalies between the registered weights and the measured weights will trigger an inspection requirement and bring the vehicle through the Port of Entry. In addition, some HDV from this group are selected at random for inspection. For these reasons care should be taken when applying the age distribution observed in our sampling campaign as it may or may not accurately reflect the fleet using this interstate system segment.

For this campaign the FEAT detectors were operated for part of the time in an elevated arrangement on guy wire stabilized scaffolding towers (4 to 4.5 m above the ground) to sample elevated exhaust stacks. Figure S4 shows the high installation with the two scaffolding towers supporting the detectors (far side) and light source (near side) mounted on top and the motor home that housed the computers and support equipment. Many HDV manufactured since 2011 have a ground level exhaust mounted between the rear wheels of the tractor and for part of the campaign the FEAT detectors were operated on the ground (0.3 m above the ground) to sample these trucks (Figure S5). The ground level setup also allows for the emissions of medium-duty vehicles (MDV) to be collected.

The High FEAT measurement required the use of additional infrared sensors that were installed on tripods downstream of the scaffolding to start the 1 second exhaust measurement with data collected on each detector channel at 100 Hz. The Low FEAT was triggered conventionally when a vehicle's tire passed through the Low FEAT IR beam, causing the reference signal to be blocked, and half a second of data was collected at 100 Hz for each measurement. The Low FEAT used a shorter sampling time to prevent the rear trailer wheels from interrupting the measurement. Exhaust thermographs were attempted only on HDV with elevated exhaust pipes with an infrared camera (Thermovision A20, FLIR Systems) for qualitatively estimating the exhaust temperatures of some of the trucks leaving the weigh station (Figure S6). The IR camera system has been previously field-calibrated allowing exhaust pipe temperatures to be estimated from the images.[36] However, this is necessarily only an estimate because it is often difficult to distinguish a truly cold pipe from one that has been shielded and our inability to image ground level exhaust pipes because of their location reduces the number of newer model year trucks observed.

Trucks with at least a valid CO measurement had their license plates and state and/or country manually transcribed. License plates for the states of California, Colorado, Idaho and Utah were matched against state registration records for non-personal vehicle information such as make, chassis model year and Vehicle Identification Number (VIN). The remaining license plates were manually matched using publically available registration data found online. All of the matched registration information was visually verified for vehicle make to eliminate, where possible, fallible registration information. VIN's for the matched trucks were decoded using the National Highway Traffic and Safety Administration's online VIN decoder that provided additional vehicle information such as model, engine size, engine model, engine manufacturer, engine horse power, fuel type and weight class which have been included in the final database available at https://digitalcommons.du.edu/feat/.[37]

Heavy and many medium-duty trucks in the United States have emission regulations that are enforced based on the year that the engine is manufactured, not when it is installed in a chassis. However, only chassis model year information is available from registration records which reports the year that the vehicle was assembled. It is not possible for us to unequivocally determine a vehicle's engine model year as that would require an inspection of every vehicles engine sticker, but past experience has shown that the engine model year on average is one year older.[9, 38]

Therefore in this paper chassis model year is reported for vehicle age and the engine model year, for regulation purposes, is assumed to be one year older (i.e. a 2012 chassis model year is estimated to have a 2011 engine).

## RESULTS AND DISCUSSION

The 2020 Perry Port of Entry campaign resulted in 1694 measurements from HDV (1591, class 7 and 8 with gross vehicle weight (gvw) > 26000 lbs) and MDV (103, gvw < 26000 lbs) with the majority of measurements collected during daylight hours (~28 hrs). As such, we intend to only discuss the results from the HDV (Table S1 has the measurement summary for the MDV). The FEAT remote sensor was operated in the elevated configuration for ~22 hours and in the ground level configuration for ~10 hours. Vehicles from 37 different states and Canada were sampled with the largest numbers from Utah (35.5%) and Idaho (13.9%) (Table S2). The Utah plated fleet is 2.4 years older than the Out of State fleet which has a higher percentage of 3 year old and newer trucks (49% versus 36%) indicative of the influence of long-haul trucks, while the Utah fleet has almost double (31% versus 16%) the number of HDV model year 2010 and older (Figure S7).

Table 1 provides a summary of fleet fuel specific emission averages for the High and Low setups as well as for the entire HDV fleets. Uncertainties are standard error of the mean determined using the daily measurements (see supporting information). As previously mentioned HDV equipped with ground level exhaust are generally only found on vehicles manufactured since 2011 allowing for a high percentage of these vehicles to be powered by engines equipped with $NO_x$ after-treatment systems. If you compare the fuel specific $NO_x$ emissions in Table 1 between the High and Low measurement sets you will see that they are 56% lower for the HDV

Table 1. Heavy-duty Vehicles Data Summary.

| FEAT | High | Low | All |
|---|---|---|---|
| Number of Measurements | 1053 | 538 | 1591 |
| Mean gCO/kg of fuel | 7.0 ± 1.8 | 3.4 ± 22.8 | 5.8 ± 1.5 |
| Mean gHC/kg of fuel | -2.5 ± 0.4 | 4.6 ± 2.5 | -0.08 ± 0.07 |
| Mean gNO/kg of fuel[a] | 14.2 ± 1.0 | 6.2 ± 0.8 | 11.5 ± 1.3 |
| Mean $gNH_3$/kg of fuel | 0.009 ± 0.009 | 0.23 ± 0.02 | 0.08 ± 0.06 |
| Mean $gNO_2$/kg of fuel[b] | 0.7 ± 0.1 | 0.6 ± 0.1 | 0.67 ± 0.09 |
| Mean $gNO_x$/kg of fuel[b] | 22.5 ± 1.4 | 9.9 ± 1.4 | 18.5 ± 2.0 |
| Mean IR %Opacity | 0.7 ± 0.1 | 0.4 ± 0.3 | 0.6 ± 0.1 |
| Mean Chassis Model Year | 2012.6 | 2017.4 | 2014.2 |
| Mean Speed (mph) | 27.9 | 30.9 | 28.9 |
| Mean Acceleration (mph/s) | 0.3 | 0.01 | 0.2 |
| Mean STP(skw/tonne)[c] | 6.8 | 4.4 | 6.0 |
| Roadway Slope (degrees) | 0° | 0° | 0° |
| Mean Temperature (°C) | 3.9 | 3.6 | 3.8 |

[a]Grams of NO. [b]Grams of $NO_2$. [c]Scaled Tractive Power.

measured with ground level exhaust. However, that vehicle grouping is also approximately five years newer on average (2017.4 vs 2012.6) reflecting the higher percentage of newer trucks.

Figure 1 is a bar chart for the mean fuel specific $NO_x$ emissions (left axis) versus chassis model year for the HDV measured at the Perry Port of Entry. Each bar is apportioned with the open portion showing the contribution to the total $NO_x$ emissions from NO and the solid portion the contribution from $NO_2$. The uncertainties plotted are standard error of the mean determined from the daily measurements. The solid black line drawn between chassis model years 2011 and 2021 represents the homologous $NO_x$ certification standard derived from the Portable Emissions Measurement (PEMS) on-road enforcement limit of 0.35 $gNO_x$/brake-horsepower hour (bhp-hr, 0.47 $gNO_x$/kWh) assuming 0.15 kg of fuel is consumed per bhp-hr. Keep in mind that not all of the 2011 and newer HDV are certified to this emission standard due to manufacturer emission credits earned as part of the Family Emission Limit regulations and the line only applies to the HDV that were certified to the 0.2 $gNO_x$/bhp-hr (0.26 $gNO_x$/kWh) standard.[39] The dashed line shows the fleet percentage of the Utah HDV (right axis) by model year and the 1998 chassis model year includes 1998 and all older models.

The $NO_2$ contribution at the tailpipe is small as shown with the majority of the $NO_x$ emissions contributed by the engine out NO emissions. The $NO_x$ emissions by chassis model year trends are distinguished by two relatively stable regions of emissions linked with a short transition between the two. Starting with the newest HDV in Figure 1, 2017 and newer models form the first group with the lowest $NO_x$ emissions that are similar within the measurement uncertainties, indicating little to no emissions deterioration on average over the five year period. However, emission factors for this group are still approximately 3 times higher than the PEMS on-road standard. From 2016

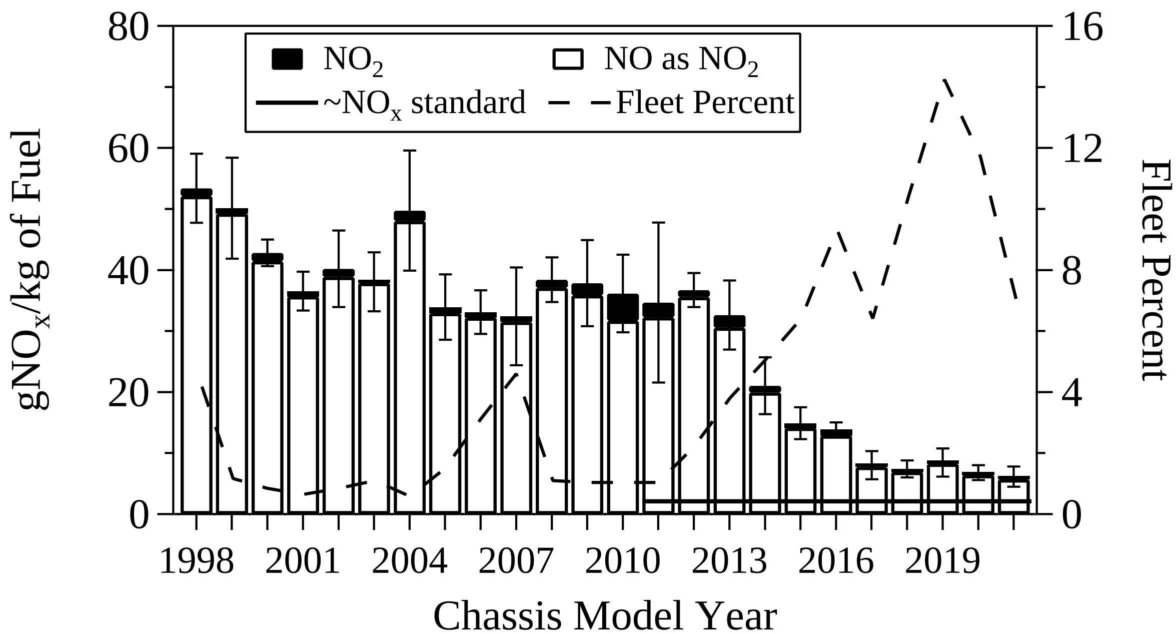


Figure 1. HDV $gNO_x$/kg of fuel (total bar height, left axis) versus chassis model year. The fraction of the total $gNO_x$/kg of fuel is divided between the gNO/kg of fuel plotted as $gNO_2$/kg of fuel (open) and the $gNO_2$/kg of fuel (solid). Uncertainties are standard error of the mean calculated from the daily means. The $NO_x$ standard is for a reference only and is calculated for engines certified to the 0.2 $gNO_x$/bhp-hr standard assuming a PEMS on-road enforcement limit of 0.35 $gNO_x$/bhp-hr and 0.15 kg of fuel/bhp-hr (~2.1 $gNO_x$/kg of fuel). Dashed line is the Utah HDV fleet percentages (right axis) by model year. The 1998 chassis model year includes 1998 and older models.

to 2013 chassis model year trucks the $NO_x$ emission levels increase quickly to a second and significantly higher $NO_x$ emissions level. In the second group, there are no real differences in mean emissions between the 2013 and 2001 chassis model year trucks. At this site and under winter conditions chassis model year 2011 to 2013 HDV have on average completely lost any previous benefit gained from their $NO_x$ after-treatment systems. A caveat is that the decreasing number of trucks in these older chassis model years increases their measurement uncertainty.

As previously mentioned there are no HDV emission measurements with identified chassis model years that have been collected during the winter months for a direct comparison. Our most recent HDV measurements were collected in the spring of 2017 at two California weigh stations (Peralta, elev. 104 m, on CA-91 in the South Coast Air Basin and Cottonwood, elev. 132 m, on I-5 near Redding, CA).[8, 40] The Peralta, CA data include both elevated and ground level exhaust measurements while the Cottonwood, CA measurements were limited to only HDV with elevated exhausts. Figure 2 graphs the fuel specific $NO_x$ emissions by chassis model year comparing the 2020 Utah and the two 2017 California HDV measurements. The uncertainties are standard error of the mean determined from the daily measurements. The differences in this comparison are obvious as both California measurements show a significantly slower increase in $NO_x$ emissions between the newest and oldest HDV. Bear in mind when the California studies were conducted and for the same chassis model year the HDV measured in Utah are 3.5 years older.

Driving mode differences between the sites are seen in higher average speeds at the Utah site (28.9 mph, 0.17 mph/sec), higher average accelerations at the Peralta, CA site (22.5 mph, 1.0 mph/sec) and the lowest speeds and accelerations are at the Cottonwood, CA site (11.9 mph, 0.16 mph/sec). Using scaled tractive power (STP) to categorize the driving mode at each site results in loads experienced at the Utah site (6 skw/tonne) falling between the two California sites (Peralta 8.6 skw/tonne and Cottonwood 3.5 skw/tonne) (Figure S8).[41] The influence of STP on fuel specific $NO_x$ emissions is not strong for any of the sites within the uncertainties of the measurements, and the site with the highest loads (Peralta, CA) has the lowest $NO_x$ emissions (Figure S9). However,

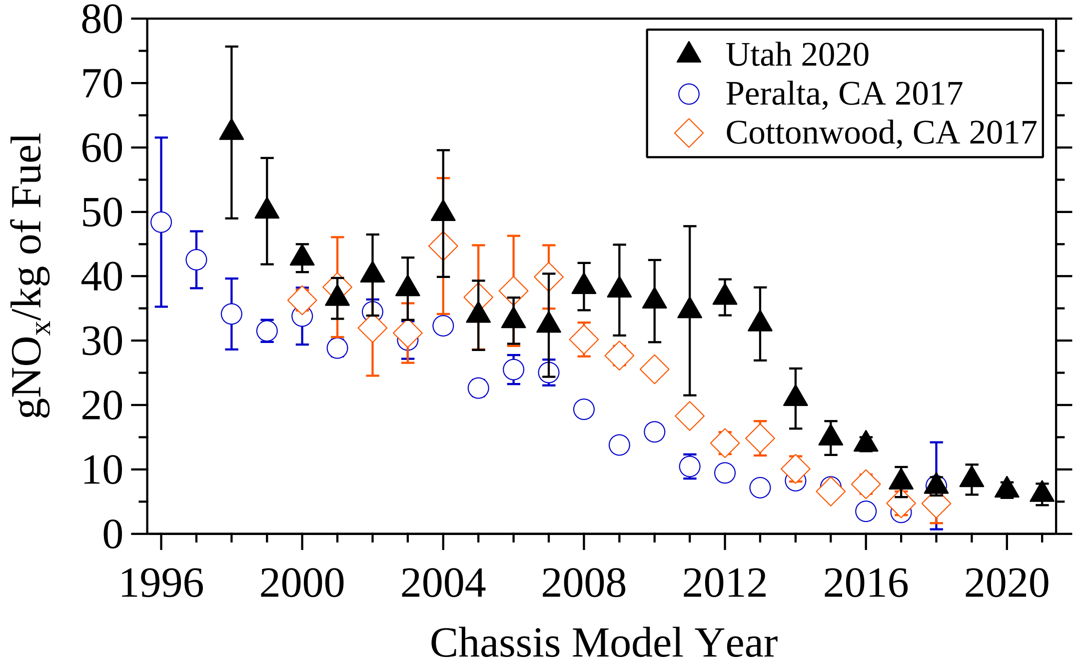


Figure 2. Heavy-duty gNO$_x$/kg of fuel versus chassis model year shown for the 2020 Utah measurements (triangles) and the 2017 California measurements at the Peralta (circles, Haugen et al., Environ. Sci. Tech. 52, 2018) and Cottonwood (diamonds, Haugen and Bishop, Environ. Sci. Tech. 52, 2018) weigh stations. Uncertainties are standard error of the mean calculated from the daily means.

since this type of plot is not normalized for vehicle age, the higher NO$_x$ emissions seen at Cottonwood for the 5 skw/tonne bin may be a result of age and not driving mode related as the majority of measurements are concentrated in that bin. It is unlikely that driving mode can explain the differences observed between the three sites.

Figure 3 is a box and whisker plot comparing the fuel specific NO$_x$ emissions and their distribution by chassis model year for HDV from the Utah (left), Cottonwood CA (center) and Peralta CA (right) measurements. For chassis model years older than 2014 we have grouped

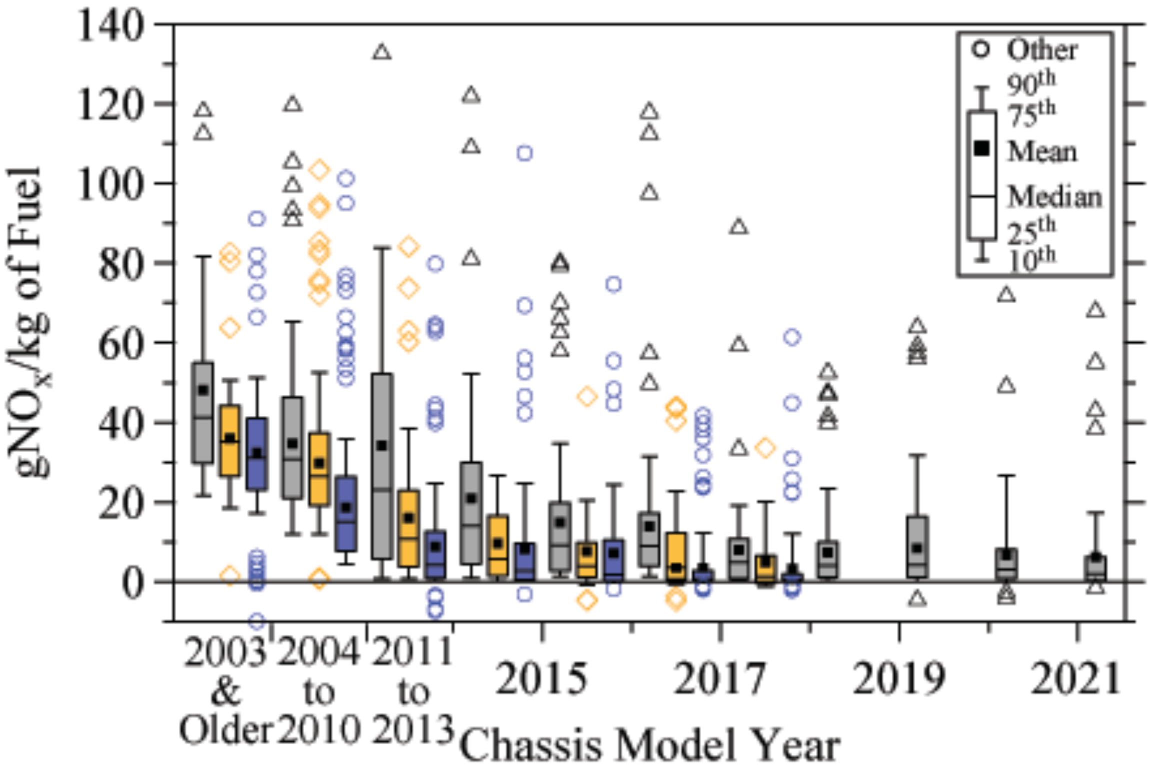


Figure 3. Box and whisker plot comparing the fuel specific $NO_x$ emissions by chassis model year for HDV measured in Utah (left, grey), Cottonwood CA (center, orange, Haugen and Bishop, Environ. Sci. Tech. 52, 2018) and Peralta, CA (right, blue, Haugen et al., Environ. Sci. Tech. 52, 2018). The box defines the $25^{th}$, $50^{th}$, and $75^{th}$ percentiles with the whiskers extending from the $10^{th}$ to the $90^{th}$ percentile. The symbols are measurements that are farther from the median than 1.75 times the whisker end. The mean for each group is plotted as the solid square.

together multiple model years by technology class in order to increase the number of measurements. The box defines the $25^{th}$, $50^{th}$, and $75^{th}$ percentiles with the whiskers extending from the $10^{th}$ to the $90^{th}$ percentile. The symbols are measurements that are farther from the median than 1.75 times the whisker end and the mean emissions for each group are plotted as filled squares.

The box and whisker plot highlights the skewed nature of the emissions distributions for all of the chassis model years. In general as the mean emissions increase so does the size of the distributions interquartile range and the extent of the highest emitters. While the mean $NO_x$ emissions for the 2011 to 2013 HDV indicate a lack of $NO_x$ reduction capability from the after-treatment systems the 10$^{th}$ percentiles graphed in Figure 3 show that there are still vehicles with functioning SCRs resulting in $NO_x$ emissions at or very close to zero. Only for 2010 and older HDV (pre-SCR) does the 10$^{th}$ percentile rise above the zero line.

$NO_x$ emissions temperature effects. Multivariate regression analysis identified the obvious connection between $NO_x$ emissions and model year as already shown in Figures 1 - 3 (see supporting information). Additionally, only exhaust pipe temperature was found to be a significant predictor of HDV $NO_x$ emissions. While we do not believe we can unequivocally assign temperatures influence on $NO_x$ emissions with a single data set, because of the large age range of HDV in the Utah fleet and the subsequent differences in engine management systems, this data does allow the opportunity to discuss the relative magnitude of the possible effects. As designed, the Utah measurements were conducted at lower ambient temperatures (-7 to 10°C) than the California measurements (11.5 - 20°C) to investigate HDV $NO_x$ emission performance at these lower temperatures. The ambient temperature difference is also reflected in the IR thermographs collected with average exhaust pipe temperatures 18°C and 16°C lower in Utah compared to Peralta and Cottonwood, CA, respectively (Figure S10).

To gauge the role of temperature, we will first focus on 3 year old and newer trucks shown in Figure 3. This selects 2018 - 2021 chassis model year vehicles in Utah (687 measurements, 7.19 ± 0.97 $gNO_x$/kg of fuel) and 2014 - 2017 chassis model year vehicles in California (716 Peralta measurements, 5.34 ± 0.31 $gNO_x$/kg of Fuel and 348 Cottonwood measurements, 7.5 ± 4.5

$gNO_x$/kg of fuel). All of these HDV will have fully electronically controlled engines that will be expected to adjust engine operation for any temperature and pressure changes. The interquartile range and mean $NO_x$ emissions are similar across the three sites with the exception being the first two model years (2017 and 2016) observed at Peralta, CA which are exceptionally low and account for the 26% differences in the means. The frequency and extent of the measurements beyond the 90$^{th}$ percentile is similar between the Utah and the Peralta CA measurements while the Cottonwood measurements are lower on both counts.

Using the elevated exhaust pipe thermograph temperatures Figure 4 is a plot of fuel specific $NO_x$ emissions versus exhaust pipe temperature (°C) for the 3 year old and newer HDV at each site. The lines are linear least squares fits to each set of points and the uncertainties are standard error of the mean determined from the daily measurements. All three sites show decreasing $NO_x$ emissions with increasing exhaust pipe temperature with slopes of -0.09, -0.08 and -0.06 $gNO_x$/kg of fuel/°C for Utah, Peralta, and Cottonwood, CA, respectively. While not a direct measurement of SCR temperature the exhaust pipe temperatures support the expected improvement in $NO_x$ conversion efficiency as SCR temperatures increase (Figure S1). If the Utah HDV had comparable exhaust pipe temperatures to the Peralta CA fleet (18°C higher) mean fuel specific $NO_x$ emission factors on average would be predicted to decrease to 5.6 $gNO_x$/kg of fuel within the uncertainties of the Peralta measurements (5.34 ± 0.31 $gNO_x$/kg of Fuel). Ascribing all of the differences between the Utah and Peralta, CA mean $NO_x$ emissions to the lower exhaust pipe temperatures establishes an upper limit for the newest HDV for these operating temperatures of ~25%.

Comparisons of the Utah and Peralta, CA emissions using a quantile - quantile plot show distribution similarities at the low and high emission ends with the shift to higher $NO_x$ emissions occurring in the middle percentiles (Figure S11). This is consistent with the hypothesis that lower

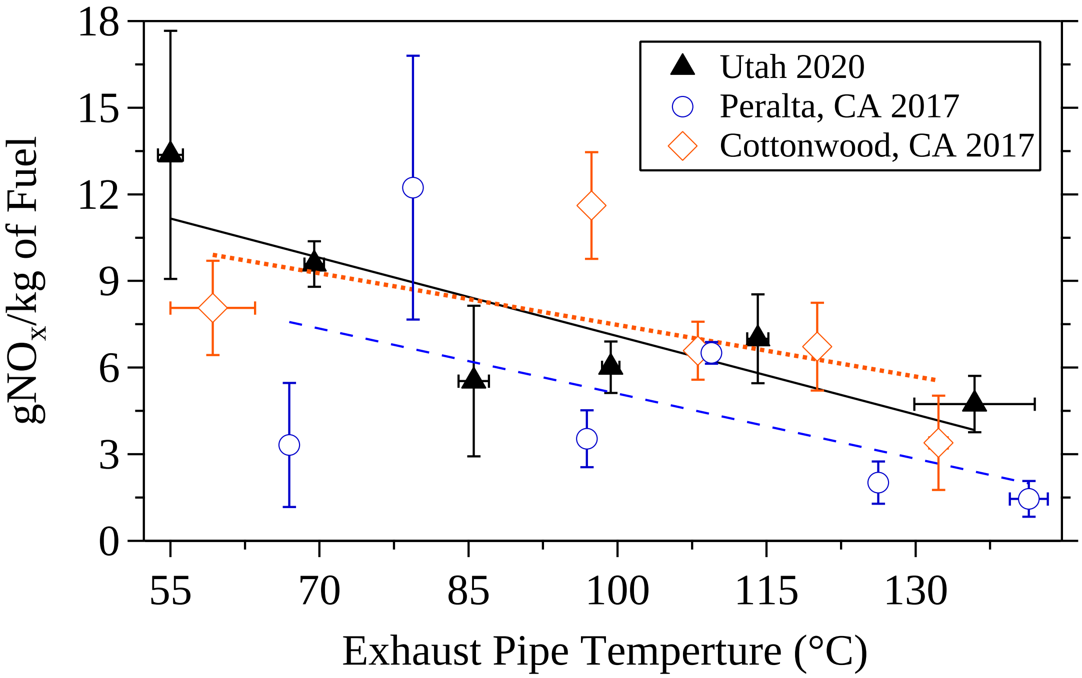


Figure 4. Fuel specific $NO_x$ emissions versus exhaust pipe temperature (°C) for 3 year old and newer HDV in the Utah (2018 - 2021) and California (2014 - 2017) data sets. The solid line is a least squares best fit line to the Utah data (triangles, slope = -0.09, $R^2 = 0.68$), the dashed line is fit to the Peralta, CA data (circles, slope = -0.08, $R^2 = 0.28$, Haugen et al., Environ. Sci. Tech. 52, 2018) and the dotted line is fit to the Cottonwood, CA data (diamonds, slope = -0.06, $R^2 = 0.31$, Haugen and Bishop, Environ. Sci. Tech. 52, 2018). Uncertainties are standard error of the mean determined from the daily measurements.

ambient temperatures have lowered the SCR conversion efficiency (Figure S1) rather than increased the number of catalysts that are inoperative. However, the fact that we observe high $NO_x$ emissions in the newest HDV at all the sites, an observation also reported by other researchers, suggests an issue that involves more than temperature differences.[42]

There are no significant differences between the Utah (7.19 ± 0.97 $gNO_x$/kg of fuel) and Cottonwood, CA (7.5 ± 4.5 $gNO_x$/kg of fuel) means for the newest vehicles, though the Cottonwood uncertainties are very large. The Cottonwood measurements are different in that the higher means are not the result of a larger number of high emission outliers but an increase in emissions between the 25$^{th}$ and 85$^{th}$ percentiles (Figure S12). It is unclear if this result is due to how the two methods collect the emissions (averaged over ~8 sec of driving for the OHMS method used at Cottonwood versus 0.5 to 1 sec with FEAT in Utah and Peralta, CA) or whether they are somehow influenced by the lower load and slower driving speeds at Cottonwood.[43] However, the relationship between $NO_x$ emissions and exhaust pipe temperature is not too dissimilar from that recorded at the other two sites.

We believe the older mechanically controlled Utah trucks (2003 & older) can also be used to estimate potential ambient temperature effects on $NO_x$ emissions after accounting for the influence of altitude. These trucks generally do not have the ability to effectively compensate for altitude changes and while the Perry Port of Entry is within the elevation limits for Federal emission performance (less than 1676 m) it is still approximately 1 km higher in elevation than both of the California sites. The box and whisker plot in Figure 3 shows a $NO_x$ mean emission difference of 25 and 33% between the Utah (48.1 ± 2.7 $gNO_x$/kg of fuel) and California (Cottonwood 36.0 ± 2.2, Peralta 32.4 ± 0.2 $gNO_x$/kg of fuel) emissions for 2003 & older HDV. Normalizing the model year distribution between the Utah and California fleets slightly lowers the Utah mean used for a comparison to 45.6 $gNO_x$/kg of fuel and 45.2 $gNO_x$/kg when matching the Cottonwood or Peralta model year distributions, respectively. This leaves a difference of 9.6 and 12.8 $gNO_x$/kg of fuel when compared to the normalized Utah fleet mean. Previous research has shown that altitude increases $NO_x$ emissions approximately 6.3 $gNO_x$/kg of fuel/km in these trucks, which when applied accounts for three quarters of the difference with Cottonwood and a little more than half of the difference at Peralta.[44] This leaves aging (3.5 year difference between the measurement dates) and temperature effects to possibly account for the remaining differences (2.2 out of 36 $gNO_x$/kg of fuel at Cottonwood and 5.3 out of 32.4 $gNO_x$/kg of fuel at Peralta) and assuming an equal contribution between these two factors suggests only a minor temperature effect (less than 10%) on these vehicles' $NO_x$ emissions.

The previous tunnel and near road measurements have observed $NO_x$ increases in the winter from HDV of 20% to 50% depending on the study.[16-19] Our data suggests a temperature dependence on the order of 25% for the newest vehicles and <10% for the oldest. Trying to estimate a temperature effect on the remaining vehicles is not possible with only one data set but the percentage increases in $NO_x$ emissions observed in Utah come in at the lower range of those reported by the earlier researchers.

<u>Emission modeling comparison.</u> Agencies in the U.S. outside of California rely on the Environmental Protection Agencies MOVES computer model for on and off-road vehicle emissions to include in their inventories.[45] Using the most recent version of this model, MOVES3, we calculated the tailpipe running emissions (CO, THC, NO, $NO_x$ and $CO_2$) for a December 2020 Utah HDV fleet (vehicle types 46, 47 and 49). The emissions was supplied with Utah Department of Transportation data for speeds and vehicle miles traveled for an urban restricted access road type and the meteorology profile from MOVES3 for Box Elder county (county of the Perry Port of Entry). MOVES3 grams/day running emissions were converted into fuel specific molar emissions for comparison (see the supporting information). Figure 5 compares the fuel specific $NO_x$ emissions between the Utah 2020 measurements (HDV Class 7 & 8) and the MOVES3 estimates for Box Elder county Utah. Uncertainties for the Utah measurements are standard error

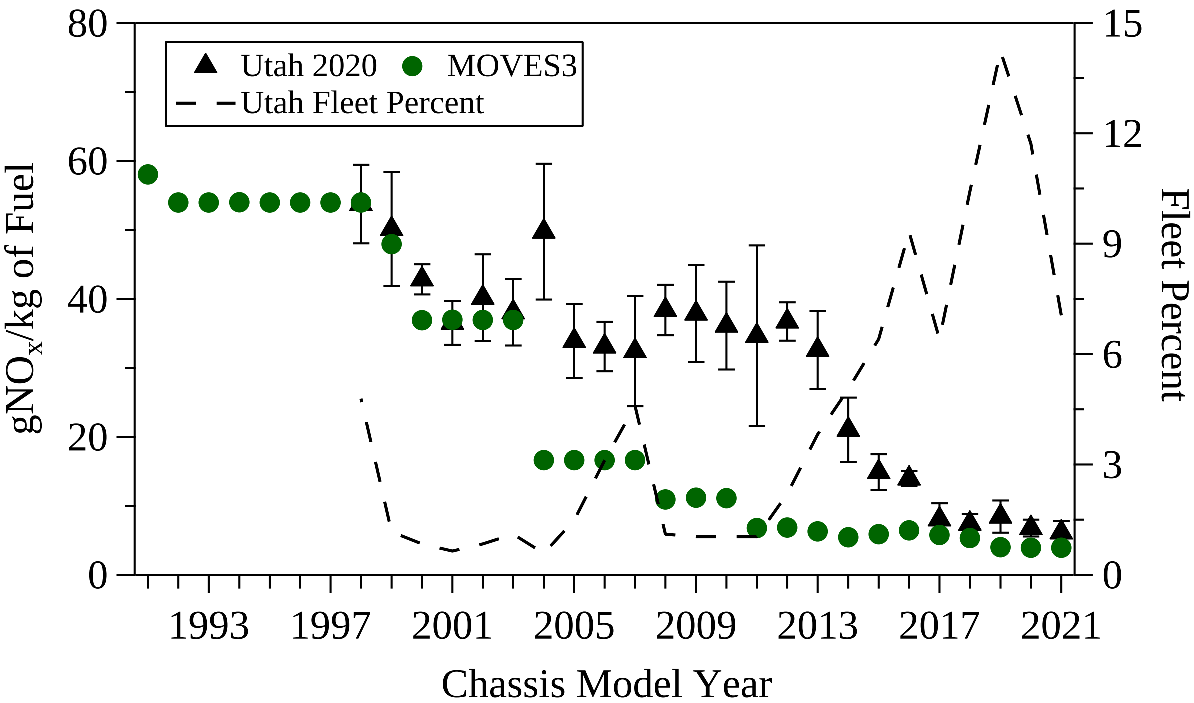


Figure 5. Fuel specific $NO_x$ emissions versus chassis model year for the Utah measurements and the MOVES3 estimates for Box Elder County. Uncertainties are standard error of the mean calculated using the daily means and 1998 models includes 1998 and older model years. The Utah fleet percent by chassis model year is the dashed line and is plotted against the right axis.

of the mean determined using the daily means and all HDV 1998 and older are included in the 1998 measurement.

The measurements have higher $NO_x$ emissions for all model years except for the 2003 and older chassis model years where there is good agreement. Table 2 compares the means for the CO and $NO_x$ emissions using the observed Utah age distribution from Figure 5 for the MOVES3 estimates. Uncertainties for the Utah measurements are standard error of the mean determined

Table 2. Comparison of the Utah class 7 & 8 HDV fleet measurements with the MOVES3 estimated mean emissions.[a]

| Data Source | Fleet gCO/kg of Fuel | Fleet $gNO_x$/kg of Fuel | Glider Kit gNOx/kg of Fuel | 2017 & Newer gNOx/kg of Fuel |
|---|---|---|---|---|
| Utah Measurements | 5.8 ± 1.5 | 18.5 ± 2.0 | 42.3 ± 4.2 | 7.4 ± 0.8 |
| MOVES3 Box Elder County | 3.3 | 10.4 | 37.3 | 4.5 |

[a]All of the MOVES3 estimated means have been calculated from their chassis model year emission factors using the Utah fleet model year distribution.

from the daily measurements. MOVES3 mean estimates under-predict the CO and $NO_x$ emissions by a factor of 1.8 though the CO emission differences are almost within the one sigma uncertainties. Figure S13 shows the Utah fleet weighted percent difference versus chassis model year for the 8.1 $gNO_x$/kg of fuel difference between the Utah and the MOVES3 means. Major differences accumulate from the largest fleet percentages in chassis model years 2019, 2016 and 2007 but 46% of the difference occurs between model years 2012 - 2016.

The disagreement for the $NO_x$ means is actually larger than it appears because MOVES3 includes significantly more Glider Kit trucks, typically new chassis vehicles with pre-control engines installed and therefore higher $NO_x$ emissions, than found in the measurements. Using the VIN decoded information we were able to identify 23 Gliders out of 1591 HDV (1.4%, factor of 2.3 less than MOVES3 (3.3%)) and for 2017 & newer HDV they account for only 1.1% of the Utah HDV (factor of 3.9 less than MOVES3 (4.3%)) though the $NO_x$ emission factor comparison is very similar (Table 2 and Figure S14). This increases the MOVES3 $NO_x$ emission estimates by 32%.

While less important in the mean calculations, because of their lower numbers, it is still important to ask why the 2011 - 2013 HDV, on average, show no benefit from low $NO_x$ certification standards. Figure 3 shows that this model year grouping has the largest interquartile range observed indicating that some HDV in this group still benefit from functioning after-treatment systems. However, this group also shows the highest $90^{th}$ percentile level suggesting even more HDV have after-treatment systems that are either not functioning or performing very poorly. Copper zeolites are susceptible to Sulphur poisoning and while low Sulphur diesel fuel in the U.S. is limited to 15ppm over these trucks lifetime (8 to 10 years) they have still been exposed to a significant quantity of Sulphur simply due to the number of gallons of fuel they have used which may contribute to their reduced SCR conversion efficiencies.[46, 47]

In addition previous research in California found premature emissions deterioration was occurring in some SCR catalyst leading to a major manufacturer (Cummins) to voluntarily recall a number of HDV engine families from chassis model years 2011 - 2016.[8, 48] Since we do not have information to precisely identify the affected vehicles, nor do we know what the repair status of any of the recalled vehicles are, we have taken a simplistic and broad brushed look at the possible effects of this deterioration on $NO_x$ emissions. We do this by comparing the Utah fleet $NO_x$ emissions with and without vehicles equipped with Cummins engines for the effected model years. Figure S15 is a graph of fuel specific $NO_x$ emissions versus chassis model year for all of the class 7 & 8 HDV observed during the Utah campaign for 2011 and newer chassis model year vehicles, compared against the same fleet minus the HDV with Cummins engines. Within the uncertainties there are no statistically significant changes, however, chassis model years 2012 and 2013 show noticeable emission reductions, again suggesting catalyst deterioration with increasing vehicle age is a factor in the high $NO_x$ emissions observed in the 2011 - 2013 models.[8]

To provide some final context we want to point out that sophisticated exhaust after-treatment systems are still in their infancy in HDV. It is easy to forget that in light-duty vehicles oxidation catalysts were first introduced in the 1970's and three-way catalyst followed in the early 1980's. However, it was not until the late 80's and early 90's that three-way catalyst deterioration was dramatically reduced through the development of advanced wash coats.[49] Effective $NO_x$ emission control would take until the introduction of Tier II / LEV II vehicles in 2009 more than 30 years after the first catalytic converters were developed.[50] The fact that early generation SCR systems in HDV have experienced deterioration issues is likely to be expected and the observation that the five newest model year trucks in our measurements show $NO_x$ emissions stability is a promising result indicating rapid improvement.

ASSOCIATED CONTENT

**Supporting Information**. The following files are available free of charge at https://pubs.acs.org. Catalyst $NO_x$ conversion percent versus inlet temperature. Satellite images showing the location and layout of the Perry Port of Entry. Ground level photograph of the Perry Port of Entry. Photograph of the elevated emissions sensing setup. Photograph of the ground level emissions sensing setup. An IR thermograph of an elevated HDV exhaust pipe. Fleet percent comparison for Utah and Out of State HDV. Data summary of the 103 medium-duty vehicles measured. State/Country of registration for the match medium and heavy-duty vehicles license plates. Explanation of how we calculate standard error of the mean uncertainties. Fleet percent distributions by Scaled Tractive Power for the measurements. Fuel specific $NO_x$ emissions versus Scaled Tractive Power. Multivariate regression analysis description. Exhaust pipe temperature frequencies bar chart. Quantile-Quantile plot comparing Utah fuel specific $NO_x$ emissions with Peralta, CA. Cumulative probability plot comparing Utah fuel specific $NO_x$

emissions with Cottonwood, CA. MOVES3 modeling parameters. MOVES3 emissions output for class 6, 7 and 8 trucks. MOVES3 emissions output for Glider Kit vehicles. Percent difference between the Utah measurements and MOVES3 emissions by chassis model year. Fuel specific $NO_x$ emissions by chassis model year for the Utah fleet and Utah Glider trucks. Fuel specific $NO_x$ emissions by chassis model year for the Utah fleet with and without Cummins engines.

AUTHOR INFORMATION


**Corresponding Author**

*Phone: (303) 665-4307; email: gabishop10@yahoo.com


**Author Contributions**

The manuscript was written through contributions of all authors. All authors have given approval to the final version of the manuscript.


**Funding Sources**

Funding for this research was provided by the Utah Department of Environmental Quality. Support for M. J. Haugen was provided by UK Sustainable Road Freight Transport (EPSRC: EP/R035199/1).


**Notes**

The authors declare the following competing financial interest(s): G. A. Bishop acknowledges previous receipt of patent royalty payments from Envirotest, an operating subsidiary of Opus Inspection, which previously licensed vehicle emissions testing technology developed at the University of Denver.


ACKNOWLEDGMENT

The authors thank Christopher Pennell of the Utah Department of Environmental Quality, the Utah Department of Transportation and Mr. Howard Trexler and Ms. Donnetta Ford for access to the Perry Port of Entry. Ms. Stacy Hammond, Mr. Brian Himes, Mr. Robert Dawson and Dr. Chris Ruehl for help matching the license plates. Mr. Rick McKeague III for tirelessly running and rerunning the MOVES3 model. Ms. Annette Bishop for help in acquiring repair parts for a computer that did not like the cold and Jim Moini of http://moini.net for sharing his license plate collection and the invaluable resource it is for this type of work.

## REFERENCES

1. Markets Insider, 11 incredible facts about the $700 billion U.S. trucking industry. **2019**.

2. Health Effects Institute, *Traffic-related Air Pollution: A Critical Review of the Literature on Emissions, Exposure, and Health Effects. A Special Report of the HEI Panel of the Health Effects of Traffic-related Air Pollution*; 2010; http://pubs.healtheffects.org/getfile.php?u=553.

3. IARC: Diesel engine exhaust carcinogenic. Press Release 213. International Agency for Research on Cancer. http://www.iarc.fr/en/media-centre/pr/2012/pdfs/pr213_E.pdf (Aug. 2016).

4. Office of Environmental Health Hazard Assessment; California Environmental Protection Agency, *Part B: Health risk assessment for diesel exhaust*; Sacramento, 1998; http://ww2.arb.ca.gov/sites/default/files/barcu/regact/diesltac/partb.pdf.

5. Yu, K. A.; McDonald, B. C.; Harley, R. A., Evaluation of Nitrogen Oxide Emission Inventories and Trends for On-Road Gasoline and Diesel Vehicles. *Environ. Sci. Technol.* **2021,** 55, (10), 6655-6664, DOI: 10.1021/acs.est.1c00586.

6. Koebel, M.; Elsener, M.; Kleemann, M., Urea-SCR: A promising technique to reduce $NO_x$ emissions from automotive diesel engines. *Catal. Today* **2000,** 59, (3-4), 335-345.

7. Kozawa, K. H.; Park, S. S.; Mara, S. L.; Herner, J. D., Verifying Emission Reductions from Heavy-Duty Diesel Trucks Operating on Southern California Freeways. *Environ. Sci. Technol.* **2014,** 48, (3), 1475-1483, DOI: 10.1021/es4044177.

8. Haugen, M. J.; Bishop, G. A.; Thiruvengadam, A.; Carder, D. K., Evaluation of Heavy- and Medium-Duty On-Road Vehicle Emissions in California's South Coast Air Basin. *Environ. Sci. Technol.* **2018,** 52, (22), 13298-13305, DOI: 10.1021/acs.est.8b03994.

9. Bishop, G. A.; Schuchmann, B. G.; Stedman, D. H., Heavy-Duty Truck Emissions in the South Coast Air Basin of California. *Environ. Sci. Technol.* **2013,** 47, (16), 9523-9529, DOI: 10.1021/es401487b.

10. Stanton, D., Systematic Development of Highly Efficient and Clean Engines to Meet Future Commercial Vehicle Greenhouse Gas Regulations. *SAE Int. J. Engines* **2013,** 6, 1395-1480, DOI: 10.4271/2013-01-2421.

11. Misra, C.; Collins, J. F.; Herner, J. D.; Sax, T.; Krishnamurthy, M.; Sobieralski, W.; Burntizki, M.; Chernich, D., In-Use $NO_x$ Emissions from Model Year 2010 and 2011 Heavy-Duty Diesel Engines Equipped with Aftertreatment Devices. *Environ. Sci. Technol.* **2013,** 47, (14), 7892-7898, DOI: 10.1021/es4006288.

12. Thiruvengadam, A.; Besch, M. C.; Thiruvengadam, P.; Pradhan, S.; Carder, D.; Kappanna, H.; Gautam, M.; Oshinuga, A.; Hogo, H.; Miyasato, M., Emission Rates of Regulated Pollutants from Current Technology Heavy-Duty Diesel and Natural Gas Goods Movement Vehicles. *Environ. Sci. Technol.* **2015,** 49, (8), 5236-5244, DOI: 10.1021/acs.est.5b00943.

13. Quiros, D. C.; Thiruvengadam, A.; Pradhan, S.; Besch, M.; Thiruvengadam, P.; Demirgok, B.; Carder, D.; Oshinuga, A.; Huai, T.; Hu, S., Real-World Emissions from Modern Heavy-Duty Diesel, Natural Gas, and Hybrid Diesel Trucks Operating Along Major California Freight

Corridors. *Emission Control Science and Technology* **2016,** 2, (3), 156-172, DOI: 10.1007/s40825-016-0044-0.

14. Truck and Bus Regulation. California Environmental Protection Agency Air Resources Board. https://ww2.arb.ca.gov/our-work/programs/truck-and-bus-regulation (May 2021).

15. California Air Resources Board, *Risk Reduction Plan to Reduce Particulate Matter Emissions from Diesel-fueled Engines and Vehicles*; Sacramento, CA, 2000; http://www.arb.ca.gov/diesel/documents/rrpfinal.pdf.

16. Li, X.; Dallmann, T. R.; May, A. A.; Presto, A. A., Seasonal and long-term trend of on-road gasoline and diesel vehicle emission factors mesured in traffic tunnels. *Applied Science* **2020,** 10, 2458, DOI: 10.3390/app10072458.

17. Wang, X.; Kylystov, A.; Ho, K.-F.; Campbell, D.; Chow, J. C.; Kohl, S., D.; Watson, J. G.; Lee, S.-c. F.; Chen, L.-W. A.; Lu, M.; Ho, S. S. H., *Real-World Vehicle Emissions Characterization for the Shing Mun Tunnel in Hong Kong and Fort McHenry Tunnel in the United States*; 2019; https://www.healtheffects.org/system/files/WangRR199.pdf.

18. Hall, D. L.; Anderson, D. C.; Martin, C. R.; Ren, X.; Salawitch, R. J.; He, H.; Canty, T. P.; Hains, J. C.; Dickerson, R. R., Using near-road observations of CO, NOy, and $CO_2$ to investigate emissions from vehicles: Evidence for an impact of ambient temperature and specific humidity. *Atmos. Environ.* **2020,** 232, 117558, DOI: https://doi.org/10.1016/j.atmosenv.2020.117558.

19. Saha, P. K.; Khlystov, A.; Snyder, M. G.; Grieshop, A. P., Characterization of air pollutant concentrations, fleet emission factors, and dispersion near a North Carolina interstate freeway across two seasons. *Atmos. Environ.* **2018,** 177, 143-153, DOI: https://doi.org/10.1016/j.atmosenv.2018.01.019.

20. Grange, S. K.; Farren, N. J.; Vaughan, A. R.; Rose, R. A.; Carslaw, D. C., Strong Temperature Dependence for Light-Duty Diesel Vehicle $NO_x$ Emissions. *Environ. Sci. Technol.* **2019,** 53, (11), 6587-6596, DOI: 10.1021/acs.est.9b01024.

21. Chan, E. A. W.; Gantt, B.; McDow, S., The reduction of summer sulfate and switch from summertime to wintertime PM2.5 concentration maxima in the United States. *Atmos. Environ.* **2018,** 175, 25-32, DOI: https://doi.org/10.1016/j.atmosenv.2017.11.055.

22. McDonald, B. C.; McKeen, S. A.; Cui, Y. Y.; Ahmadov, R.; Kim, S.-W.; Frost, G. J.; Pollack, I. B.; Peischl, J.; Ryerson, T. B.; Holloway, J. S.; Graus, M.; Warneke, C.; Gilman, J. B.; de Gouw, J. A.; Kaiser, J.; Keutsch, F. N.; Hanisco, T. F.; Wolfe, G. M.; Trainer, M., Modeling Ozone in the Eastern U.S. using a Fuel-Based Mobile Source Emissions Inventory. *Environ. Sci. Technol.* **2018,** 52, (13), 7360-7370, DOI: 10.1021/acs.est.8b00778.

23. Travis, K. R.; Jacob, D. J.; Fisher, J. A.; Kim, P. S.; Marais, E. A.; Zhu, L.; Yu, K.; Miller, C. C.; Yantosca, R. M.; Sulprizio, M. P.; Thompson, A. M.; Wennberg, P. O.; Crounse, J. D.; St. Clair, J. M.; Cohen, R. C.; Laughner, J. L.; Dibb, J. E.; Hall, S. R.; Ullmann, K.; Wolfe, G. M.; Pollack, I. B.; Peischl, J.; Neuman, J. A.; Zhou, X., Why do models overestimate surface ozone in the Southeast United States? *Atmos. Chem. Phys.* **2016,** 16, (21), 13561-13577, DOI: 10.5194/acp-16-13561-2016.

24. Souri, A. H.; Choi, Y.; Jeon, W.; Li, X.; Pan, S.; Diao, L.; Westenbarger, D. A., Constraining NOx emissions using satellite $NO_2$ measurements during 2013 DISCOVER-AQ Texas campaign. *Atmos. Environ.* **2016,** 131, 371-381, DOI: https://doi.org/10.1016/j.atmosenv.2016.02.020.

25. Anderson, D. C.; Loughner, C. P.; Diskin, G.; Weinheimer, A.; Canty, T. P.; Salawitch, R. J.; Worden, H. M.; Fried, A.; Mikoviny, T.; Wisthaler, A.; Dickerson, R. R., Measured and modeled

CO and NOy in DISCOVER-AQ: An evaluation of emissions and chemistry over the eastern US. *Atmos. Environ.* **2014,** 96, (0), 78-87, DOI: http://dx.doi.org/10.1016/j.atmosenv.2014.07.004.

26. Jaeglé, L.; Shah, V.; Thornton, J. A.; Lopez-Hilfiker, F. D.; Lee, B. H.; McDuffie, E. E.; Fibiger, D.; Brown, S. S.; Veres, P.; Sparks, T. L.; Ebben, C. J.; Wooldridge, P. J.; Kenagy, H. S.; Cohen, R. C.; Weinheimer, A. J.; Campos, T. L.; Montzka, D. D.; Digangi, J. P.; Wolfe, G. M.; Hanisco, T.; Schroder, J. C.; Campuzano-Jost, P.; Day, D. A.; Jimenez, J. L.; Sullivan, A. P.; Guo, H.; Weber, R. J., Nitrogen Oxides Emissions, Chemistry, Deposition, and Export Over the Northeast United States During the WINTER Aircraft Campaign. *J. Geophys. Res. Atmos.* **2018,** 123, (21), 12,368-12,393, DOI: https://doi.org/10.1029/2018JD029133.

27. Salmon, O. E.; Shepson, P. B.; Ren, X.; He, H.; Hall, D. L.; Dickerson, R. R.; Stirm, B. H.; Brown, S. S.; Fibiger, D. L.; McDuffie, E. E.; Campos, T. L.; Gurney, K. R.; Thornton, J. A., Top-Down Estimates of $NO_x$ and CO Emissions From Washington, D.C.-Baltimore During the WINTER Campaign. *J. Geophys. Res. Atmos.* **2018,** 123, (14), 7705-7724, DOI: doi:10.1029/2018JD028539.

28. Harkins, C.; McDonald, B. C.; Henze, D. K.; Wiedinmyer, C., A fuel-based method for updating mobile source emissions during the COVID-19 pandemic. *Environmental Research Letters* **2021,** 16, (6), 065018, DOI: 10.1088/1748-9326/ac0660.

29. PM-2.5 (2006) Designated Area/State Information. U. S. Environmental Protection Agency. https://www3.epa.gov/airquality/greenbook.rbtc.html (August 2021).

30. Brown, S. S.; Baasandorj, M.; Franchin, A.; Middlebrook, A. M.; Goldberger, L.; Thornton, J. A.; Dube, W. P.; McDuffie, E. E.; Womack, C.; Fibiger, D. L.; Moravek, A.; Clark, J. C.; Murphy, J. G.; Mitchell, R., Aircraft measurements to characterize polluted winter boundary layers:

Overview of twin otter flights during the Utah Winter Fine Particulate Matter Study. In *AGU Fall Meeting Abstracts*, 2017.

31. Bishop, G. A.; Starkey, J. R.; Ihlenfeldt, A.; Williams, W. J.; Stedman, D. H., IR long-path photometry, A remote sensing tool for automobile emissions. *Anal. Chem.* **1989,** 61, 671A-677A, DOI: 10.1021/ac00185a746.

32. Burgard, D. A.; Dalton, T. R.; Bishop, G. A.; Starkey, J. R.; Stedman, D. H., Nitrogen dioxide, sulfur dioxide, and ammonia detector for remote sensing of vehicle emissions. *Rev. Sci. Instrum.* **2006,** 77, (014101), 1-4, DOI: 10.1063/1.2162432.

33. Burgard, D. A.; Bishop, G. A.; Stadtmuller, R. S.; Dalton, T. R.; Stedman, D. H., Spectroscopy applied to on-road mobile source emissions. *Appl. Spectrosc.* **2006,** 60, 135A-148A, DOI: 10.1366/000370206777412185.

34. Popp, P. J.; Bishop, G. A.; Stedman, D. H., Development of a high-speed ultraviolet spectrometer for remote sensing of mobile source nitric oxide emissions. *J. Air Waste Manage. Assoc.* **1999,** 49, 1463-1468, DOI: 10.1080/10473289.1999.10463978.

35. FEAT Math II. Bishop, G. A. https://digitalcommons.du.edu/feat_publications/111 (October 2021).

36. Haugen, M. J.; Bishop, G. A., Repeat Fuel Specific Emission Measurements on Two California Heavy-Duty Truck Fleets. *Environ. Sci. Technol.* **2017,** 51, (7), 4100-4107, DOI: 10.1021/acs.est.6b06172.

37. Vehicle API. National Highway Traffic Safety Administration. https://vpic.nhtsa.dot.gov/api/ (accessed August 2021).

38. Bishop, G. A.; Schuchmann, B. G.; Stedman, D. H.; Lawson, D. R., Emission Changes Resulting from the San Pedro Bay, California Ports Truck Retirement Program. *Environ. Sci. Technol.* **2012,** 46, 551-558, DOI: 10.1021/es202392g.

39. $NO_x$ and particulate averaging, trading and banking for heavy-duty engines. In *Code of Federal Regulations*; Title 40, Section 86.007-15, 2001.

40. Haugen, M. J.; Bishop, G. A., Long-Term Fuel-Specific $NO_x$ and Particle Emission Trends for In-Use Heavy-Duty Vehicles in California. *Environ. Sci. Technol.* **2018,** 52, (10), 6070-6076, DOI: 10.1021/acs.est.8b00621.

41. U. S. Environmental Protection Agency, *Exhaust emission rates for heavy-duty on-road vehicles in MOVES3*; 2020; https://nepis.epa.gov/Exe/ZyPDF.cgi?Dockey=P1010MC2.pdf.

42. Tan, Y.; Yoon, S.; Ruehl, C. R.; Herner, J.; Henderick, P.; Montes, T.; Latt, J.; Lee, A.; Florea, E.; Lemieux, S.; Robertson, W.; Hu, S.; Huai, T., Assessment of In-Use NOx Emissions from Heavy-Duty Diesel Vehicles Equipped with Selective Catalytic Reduction Systems. *Environ. Sci. Technol.* **2021,** 55, (20), 13657-13665, DOI: 10.1021/acs.est.1c03042.

43. Bishop, G. A.; Hottor-Raguindin, R.; Stedman, D. H.; McClintock, P.; Theobald, E.; Johnson, J. D.; Lee, D.-W.; Zietsman, J.; Misra, C., On-road Heavy-duty Vehicle Emissions Monitoring System. *Environ. Sci. Technol.* **2015,** 49, (3), 1639-1645, DOI: 10.1021/es505534e.

44. Bishop, G. A.; Morris, J. A.; Stedman, D. H.; Cohen, L. H.; Countess, R. J.; Countess, S. J.; Maly, P.; Scherer, S., The effects of altitude on heavy-duty diesel truck on-road emissions. *Environ. Sci. Technol.* **2001,** 35, 1574-1578, DOI: 10.1021/Es001533a.

45. Modeling and Inventories; MOVES (Motor Vehicle Emission Simulator). U. S. Environmental Protection Agency. http://www.epa.gov/otaq/models/moves/ (October, 2014).

46. Mohan, S.; Dinesha, P.; Kumar, S., NOx reduction behaviour in copper zeolite catalysts for ammonia SCR systems: A review. *Chem. Eng. J.* **2020,** 384, 123253, DOI: https://doi.org/10.1016/j.cej.2019.123253.

47. Jiang, H.; Guan, B.; Peng, X.; Wei, Y.; Zhan, R.; Lin, H.; Huang, Z., Effect of sulfur poisoning on the performance and active sites of Cu/SSZ-13 catalyst. *Chem. Eng. Sci.* **2020,** 226, 115855, DOI: https://doi.org/10.1016/j.ces.2020.115855.

48. Cummins to recall 500,000 medium- and heavy-duty trucks due to SCR issue. Fleet Equipment. https://www.fleetequipmentmag.com/cummins-to-recall-500000-medium-and-heavy-duty-trucks-due-to-scr-issue/.

49. Shelef, M.; McCabe, R. W., Twenty-five years after introduction of automotive catalysts: what next? *Catal. Today* **2000,** 62, (1), 35-50, DOI: https://doi.org/10.1016/S0920-5861(00)00407-7.

50. Bishop, G. A.; Haugen, M. J., The story of ever diminishing vehicle tailpipe emissions as observed in the Chicago, Illinois area. *Environ. Sci. Technol.* **2018,** 52, (13), 7587-7593, DOI: 10.1021/acs.est.8b00926.

**Supporting Information For:**

Utah Wintertime Measurements of Heavy-duty Vehicle Nitrogen Oxide Emission Factors

Gary A. Bishop[†*], Molly J. Haugen[‡], Brian C. McDonald[§] and Adam M. Boies [‡]

[†]Department of Chemistry and Biochemistry, University of Denver, Denver, Colorado 80208, United States

[‡]Department of Engineering, University of Cambridge, Cambridge, United Kingdom CB2 1PZ

[§]Chemical Sciences Laboratory, National Oceanic and Atmospheric Administration, Boulder, Colorado 80305, United States of America

[*]Corresponding author: Gary A. Bishop, gbishop@du.edu

Number of pages: 19.
Number of tables: 4.
Number of figures: 15.

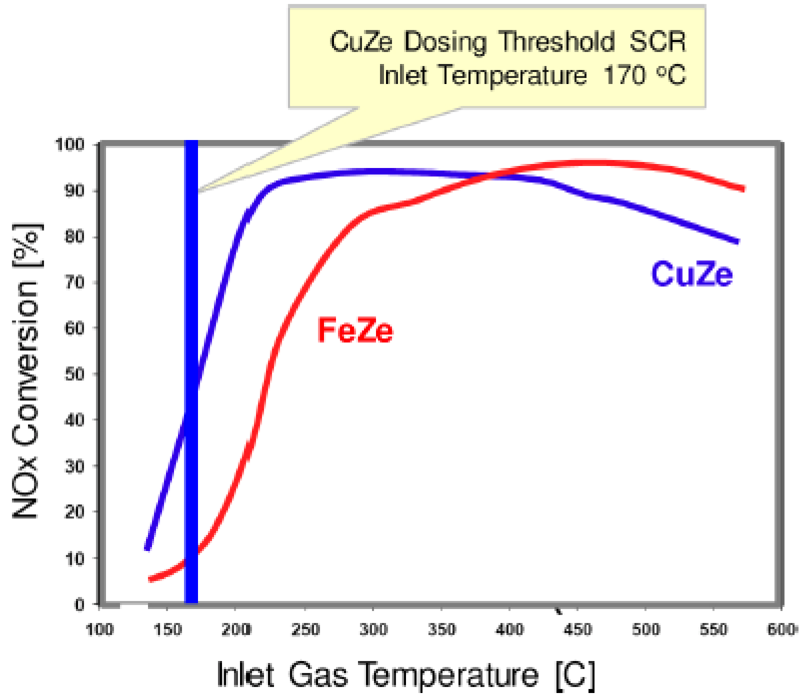


**Figure S1.** $NO_x$ conversion percent versus SCR inlet gas temperature for two substrate types of selective catalytic reduction catalyst materials (Stanton, 2013).

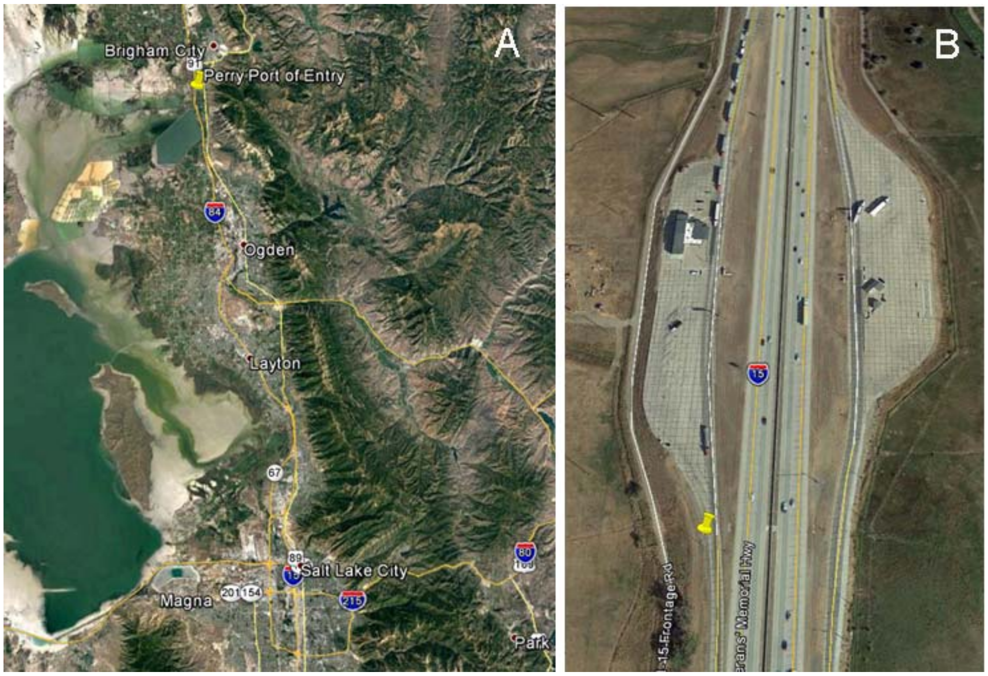


**Figure S2.** A satellite photo on the left (A) shows the location of the Perry Port of Entry north of the Salt Lake City area on Interstate 15. The satellite photo on the right provides a close up view of the layout of the Perry Port of Entry with the approximate measurement location indicated by the yellow pin on the southbound side of I-15.

**Figure S3.** View looking north toward the scales showing the Port of Entries lane arrangement. Speed limits through the port were 3mph on the west lane (left) and 20 mph on the east lane (right).

**Figure S4.** A photograph showing the scaffolding setup for measuring exhaust from trucks with elevated pipes. The light source is on the right tower and the detectors on the left. The road barrel on the far side of the highway houses the IR camera.

**Figure S5.** A photograph showing the ground level setup and the twin tripod mounted sensors used for measuring vehicle speed and acceleration.

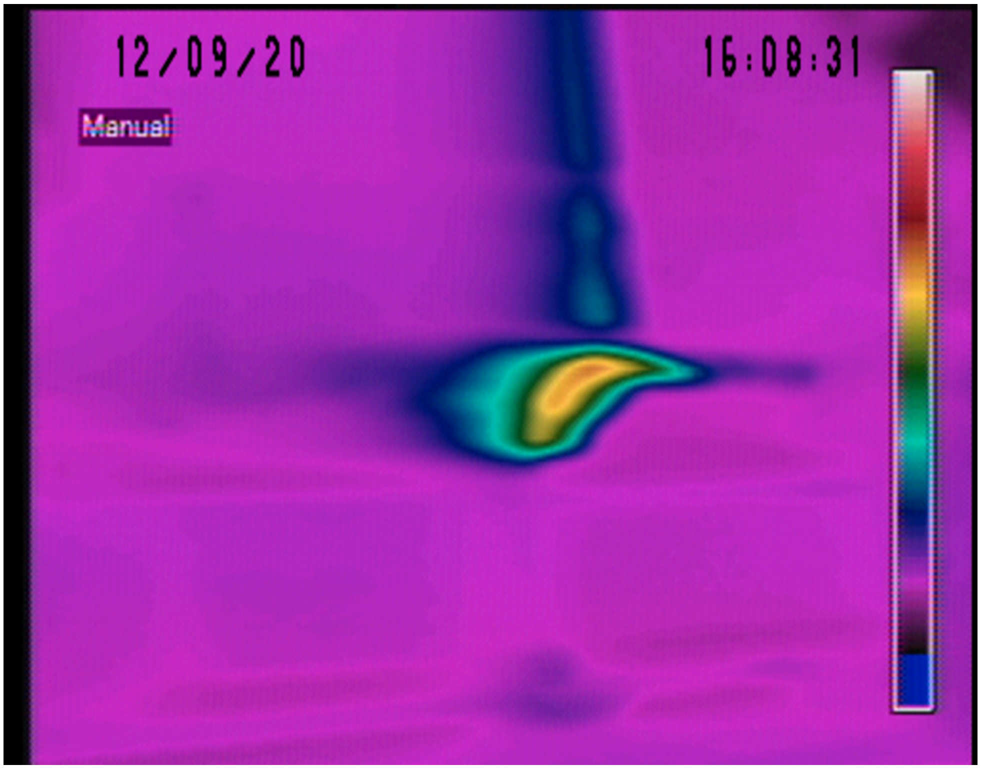


**Figure S6.** A thermal image of a truck with an elevated exhaust pipe collected on December 9th. Pipe temperature was estimated at 115° C for this truck.

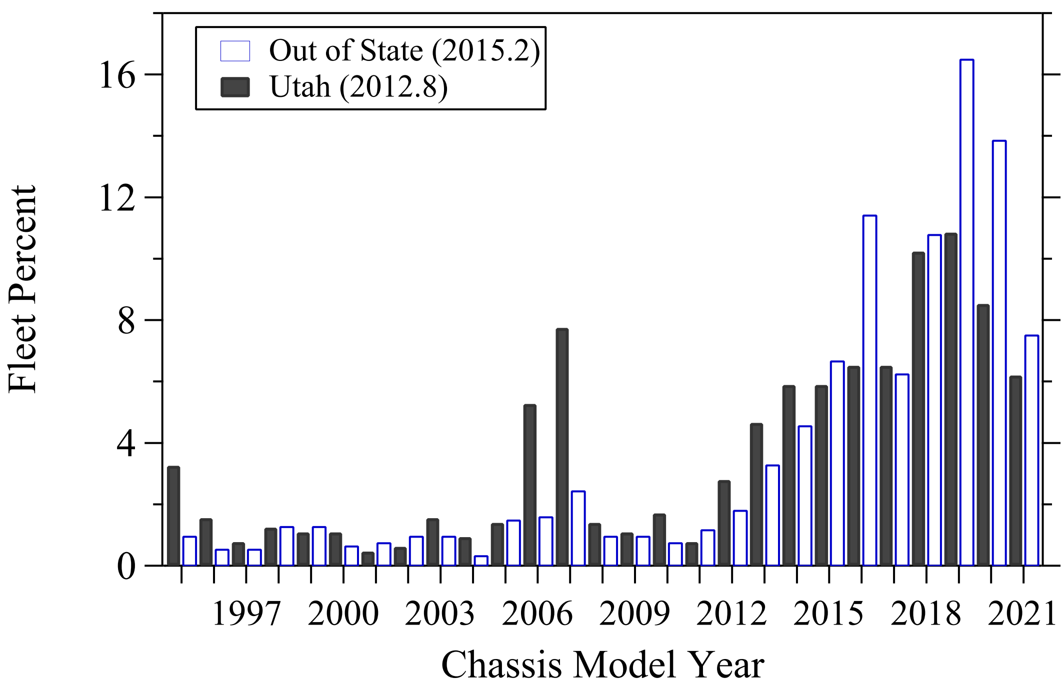


**Figure S7.** Fleet percent versus model year for the Utah plated HDV fleet and the Out of State HDV fleet.

**Table S1.** Medium-duty Vehicles Data Summary.

| | |
|---|---|
| FEAT<br>Number of Measurements | All<br>103 |
| Mean gCO/kg of fuel) | 10.7 ± 6.8 |
| Mean gHC/kg of fuel | 4.7 ± 5.1 |
| Mean gNO/kg of fuel[a] | 9.1 ± 4.9 |
| Mean $gNH_3$/kg of fuel | 0.22 ± 0.23 |
| Mean $gNO_2$/kg of fuel[b] | 0.77 ± 0.3 |
| Mean $gNO_x$/kg of fuel[b] | 14.5 ± 7.8 |
| Mean IR %Opacity | 0.6 ± 0.1 |
| Mean Chassis Model Year | 2015.2 |
| Mean Speed (mph) | 32.8 |
| Mean Acceleration (mph/s) | -0.4 |
| Mean STP(skw/tonne)<br>Slope (degrees) | 4.6<br>0° |
| Mean Temperature (°C) | 3.8 |

[a]Grams of NO. [b]Grams of $NO_2$.

**Table S2.** 2020 Perry Port of Entry matched license plates for HDV and MDV.

| State | HDV Total (Unique) | MDV Total (Unique) |
|---|---|---|
| AL | 3 | 0 |
| AZ | 8 | 0 |
| CA | 41 | 1 |
| CO | 11 | 1 |
| FL | 10 | 0 |
| GA | 6 | 0 |
| IA | 11 | 0 |
| ID | 217 (196) | 11 (10) |
| IL | 63 | 0 |
| IN | 163 (151) | 2 |
| KS | 2 | 0 |
| MD | 2 | 0 |
| MI | 6 | 0 |
| MN | 19 | 0 |
| MO | 25 | 0 |
| MS | 1 | 0 |
| MT | 13 | 1 |
| NC | 6 | 0 |
| ND | 10 | 1 |
| NE | 33 | 0 |
| NJ | 2 | 0 |
| NM | 6 | 0 |
| NV | 3 | 0 |
| NY | 4 | 0 |
| OH | 16 | 1 |
| OK | 15 | 0 |
| OR | 48 (47) | 0 |
| PA | 1 | 0 |
| RI | 1 | 0 |
| SC | 1 | 0 |
| SD | 2 | 0 |
| TN | 15 (14) | 0 |
| TX | 49 (48) | 5 |
| UT | 645 (501) | 79 (77) |
| WA | 45 | 0 |
| WI | 7 | 0 |
| WY | 8 | 0 |
| Canada | 73 | 0 |
| Totals | 1591 (1411) | 103 (100) |

How we estimate standard errors of the mean for our reported uncertainties:

Vehicle emissions from US vehicle fleets are not normally distributed, thus the assigning of uncertainties on fleet emission means involves a process that many readers may not be familiar with. Standard statistical methods that were developed for normally distributed populations, when used on a skewed distribution, result in uncertainties that are unrealistically too small due to the large number of samples. The Central Limit Theorem in general indicates that the means of multiple samples, randomly collected, from a larger parent population will be normally distributed, irrespective of the parent populations underlying distribution. Since we almost always collect multiple days of emission measurements, we use these daily measurements as our randomly collected multiple samples from the larger population and report uncertainties based on their distribution. We calculate means, standard deviations and finally standard errors of the mean for this group of daily measurements. We report the fleet weighted means for all of the emission measurements and then calculate a standard error of this weighted mean by applying the same error percentage obtained from the ratio of the standard error of the mean for the daily measurements divided by the daily measurement mean. An example of this process is provided below for the 2020 Utah $gNH_3$/kg of fuel and $gNO_x$/kg of fuel measurements. While this example is for a fleet mean we also use this technique when we report uncertainties for other statistics such as individual model years, specific fuel or technology types, and VSP. For example each model year will have its daily means averaged and then its standard error of the mean for the daily average computed and that percent uncertainty (Daily STD Error MY/Daily MY average) will be applied to that model year's mean emissions.

Utah 2020

| Date | Mean $gNH_3$/kg of fuel | Counts | Mean $gNO_x$/kg of fuel | Counts |
|---|---|---|---|---|
| 12/6/2020 | 0.0263 | 20 | 16.971 | 20 |
| 12/7/2020 | -0.0453 | 255 | 22.904 | 253 |
| 12/8/2020 | 0.0375 | 52 | 19.241 | 52 |
| 12/9/2020 | 0.0412 | 221 | 23.751 | 219 |
| 12/10/2020 | 0.0243 | 519 | 22.076 | 517 |
| 12/11/2020 | 0.2291 | 512 | 9.837 | 484 |
| | | | | |
| Average for Daily Mean | 0.0594 | | 19.13 | |
| Standard Error for the daily means | 0.0377 | | 2.12 | |
| | | | | |
| Weighted Fleet Mean | 0.0823 | | 18.45 | |
| Standard Error calculated for the fleet means | 0.0594 | | 2.04 | |
| | | | | |
| As reported in Table 1 | 0.08 ± 0.06 | | 18.5 ± 2.0 | |

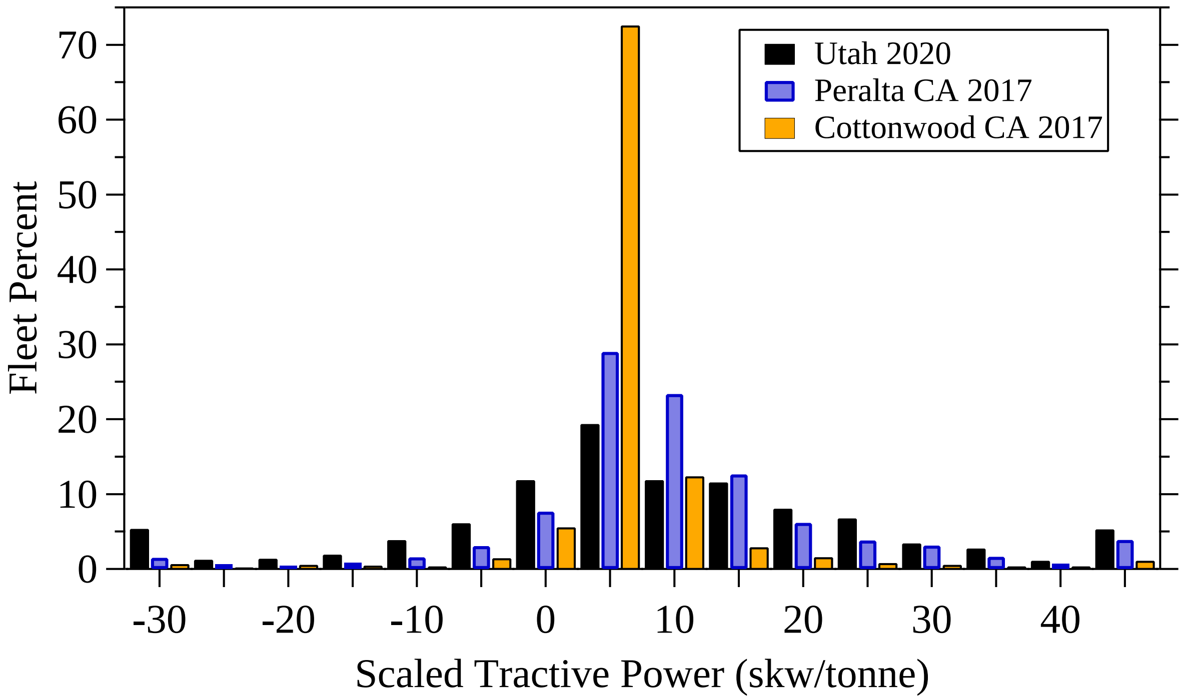


**Figure S8.** Fleet percent versus scaled tractive power bin (skw/tonne) for the 2020 Utah, 2017 Peralta CA and the 2017 Cottonwood CA HDV measurements.

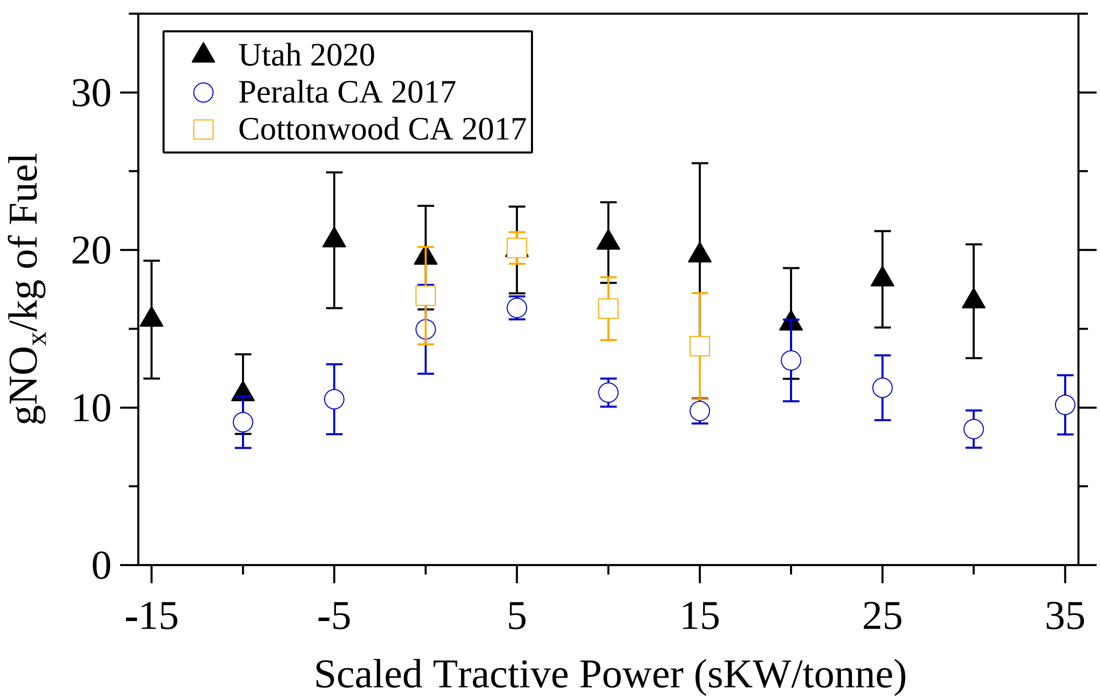


**Figure S9.** Fuel specific $NO_x$ emissions versus scaled tractive power bins for the Utah and California measurements. Uncertainties are standard error of the mean calculated using the daily means. The two endpoint bins contain all measurements above or below them and the bins have been selected for a minimum of 45 measurements.

Multivariate Regression Analysis

We perform a multivariate regression analysis using the R software package. The regression is performed on the data collected at the Utah Port of Entry. The purpose of the regression analysis is to assess whether the role of temperature exhibits statistically significant trends with $NO_x$ emission factors when controlling for other engine characteristics, including model year and engine load. Our hypothesis is that as the exhaust temperature increases, the $NO_x$ emission factor decreases. We construct the multivariate regression as follows:

$$EF_{NOx} = \beta_0 + \beta_1 \cdot age + \beta_2 \cdot STP + \beta_3 \cdot exhT$$

where:

$EF_{NOx}$ = $NO_x$ emission factor (g $NO_2$-eq/kg fuel)

$\beta_0$, $\beta_1$, $\beta_2$ = regression coefficients

age = age of engine based on chassis model year (years)

STP = scaled tractive power (skw/tonne)

exhT = exhaust pipe temperature ($^0$C)

We do not expect a-priori that the age of an engine, the scaled tractive power, and exhaust pipe temperature will be correlated with one another. Note the exhaust temperature is measured via an infrared camera, and we are only able to include in the regression analysis successful infrared image captures for trucks with high exhaust pipes. In total, 581 of the 1053 high-exhaust trucks had successful infrared image captures. None of the low-exhaust trucks are included in the regression analysis as the infrared camera was not targeted to measure the exhaust of low pipes.

Below are results of the multivariate regression ($R^2$ = 0.35, degrees of freedom = 577):

| **Coefficient** | **Value (±Std. Err)** | **t-value** | **Pr (> \| t \|)** |
|---|---|---|---|
| $\beta_0$ (intercept) | 15.4 ± 3.9 | 3.9 | 9.8e-5 |
| $\beta_1$ (age) | 1.74 ± 0.11 | 16.3 | < 2e-16 |
| $\beta_2$ (STP) | 0.045 ± 0.027 | 1.7 | 0.099 |
| $\beta_3$ (exhT) | -0.097 ± 0.038 | -2.6 | 0.011 |

The intercept indicates that for a new truck (age = 0) with no engine load (STP = 0 skw/tonne), an emission factor of 15.4 g $NO_x$/kg fuel is expected at an exhaust pipe temperature of 0 $^0$C, which is statistically significant from zero at a 99.9% confidence level. As the age of the engine increases, the emissions increase by 1.74 g $NO_x$ / kg fuel per year, and coefficient statistically significant at a 99.9% confidence level. For every $10^0$ C increase in the exhaust pipe temperature, there is a corresponding decrease in emissions by 0.97 g $NO_x$/kg fuel, and coefficient statistically significant at a 95% confidence level. Unlike the other two independent variables (age and exhT), the coefficient for scaled tractive power is not statistically different from zero at a 95% confidence level. In addition we looked at whether ambient temperature measurements recorded at the site could be used to predict the measured $NO_x$ emissions factors and found that they were not significant factor. Overall, the results of the multivariate regression largely confirm our analysis in the main text of environmental and engine variables, which indicate the importance of age/deterioration and temperature on the $NO_x$ emission factor of heavy-duty diesel vehicles.

.

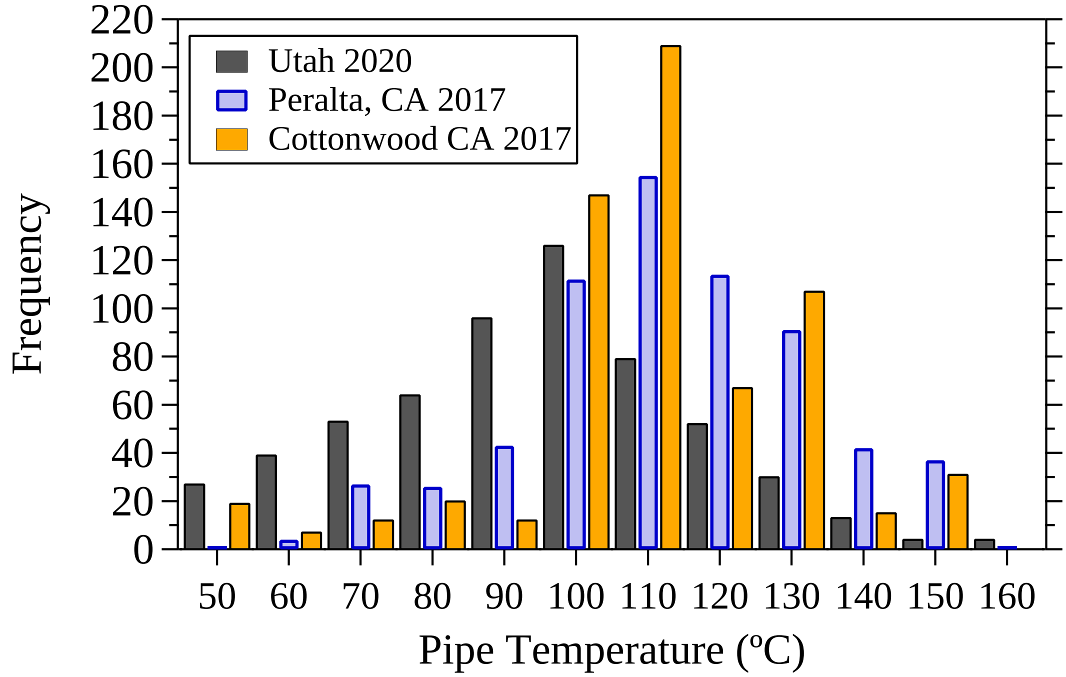


**Figure S10.** Comparison of the exhaust pipe temperature distribution determined from the infrared thermographs of elevated exhaust pipes collected during the winter 2020 Utah measurements and the spring 2017 California measurements. Mean observed temperatures were 92°C for Utah, 110°C for Peralta and 108°C for the Cottonwood measurements.

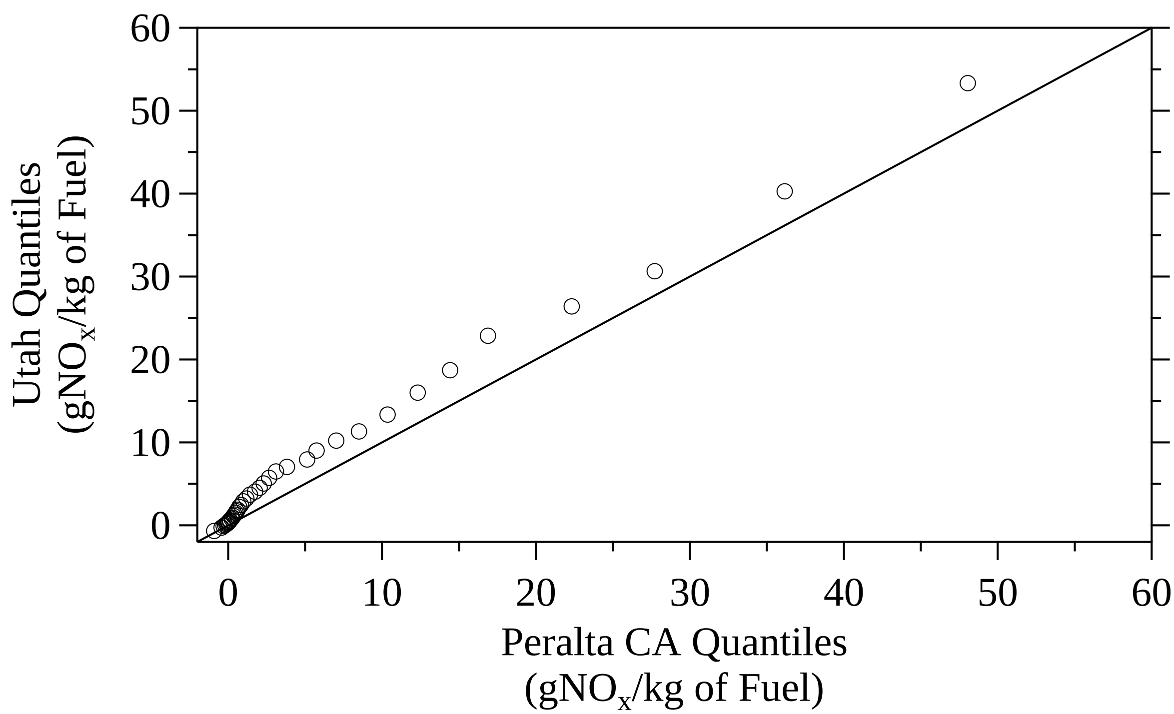


**Figure S11.** Quantile - Quantile plot of fuel specific $NO_x$ emissions for the 3 year old and newer HDV measured in Utah and Peralta CA comparing the emissions distribution. Quantiles range from the 2.5$^{th}$ to the 99$^{th}$. The solid line is a 1:1 line.

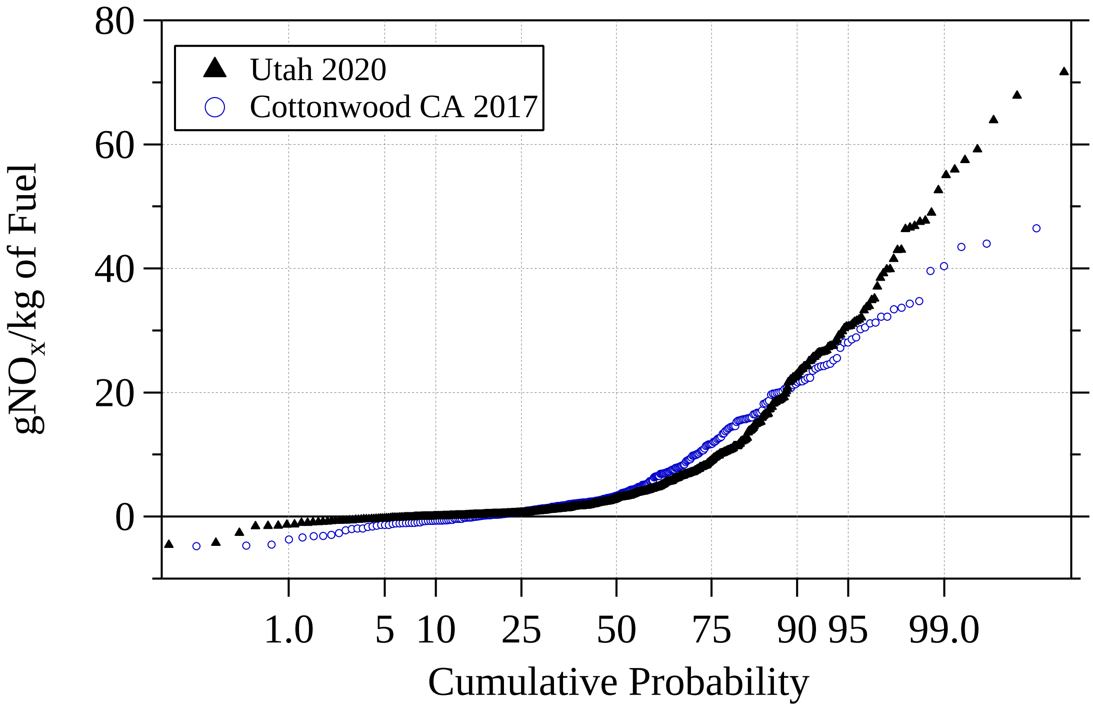


**Figure S12.** Cumulative probability plot of fuel specific $NO_x$ emissions for the 3 year old and newer HDV measured in Utah and Cottonwood CA. The x-axis has been transformed to a normal distribution. If the data sets were normally distributed they would plot as a diagonal straight line.

MOVES3 Vehicle, Fuel and Other Parameters Used

| regClassID | regClassDesc |
|---|---|
| 46 | Class 6 and 7 Trucks (19,500 lbs < GVWR > 33,000 lbs) |
| 47 | Class 8a and 8b Trucks (GVWR>33,000 lbs) |
| 49 | Glider Kit Vehicles (see EPA-420-F-15-904) |

| regClassID | sourceTypeID | sourceTypeName |
|---|---|---|
| 46, 47 | 61 | Combination Short-haul Truck |
| 46, 47 | 62 | Combination Long-haul Truck |

| fueltypeID | fuelTypeDesc | humidityCorrectionCoeff | fuelDensity |
|---|---|---|---|
| 2 | Diesel Fuel | 0.0026 | 3167 |

Model was run for December 5, 2020 and for Box Elder County (countyid=49003) and output was generated for hot running emissions for an urban restricted access road type (type 4).

Notes: MOVES3 reports NO as grams of $NO_2$ and vehicle model year output is for engine model year. We have added one year to the engine model years to convert to chassis model year.

To convert gram to moles we have used the molecular weights of 44 grams/mole for $CO_2$, 28 grams/mole for CO, 46 grams/mole for both NO and $NO_x$ and because MOVES3 reports HC emissions as measured by a flame ionization detector we have used 12 grams/mole to convert the Total Gas HC to moles of HC.

The molar ratios to $CO_2$ have been converted to fuel specific emissions using the same equations that we use to convert the FEAT measured molar ratios. We have used 860 grams Carbon per kilogram of fuel.

$$gCO/kg\ of\ Fuel = (28 * 860 * CO/CO_2) / ((1 + CO/CO_2 + HC/CO_2)*12)$$

$$gNO_x/kg\ of\ Fuel = (46 * 860 * NO_x/CO_2) / ((1 + CO/CO_2 + HC/CO_2)*12)$$

Table S3. MOVES3 Emission Output for class 6, 7 and 8 Heavy-duty Vehicles.

| Emissions in grams/day | | | | | | |
|---|---|---|---|---|---|---|
| Type 46 and 47 all sources (Class 6, 7, 8a and 8b) | | | | | | |
| Chassis MY | Atmospheric CO2 | CO | NO as NO2 | NOx | Total HC | VMT |
| 1991 | 216740.05 | 552.39 | 3750.28 | 4011.00 | 80.79 | 108.54 |
| 1992 | 105153.70 | 277.00 | 1692.12 | 1809.76 | 38.61 | 52.76 |
| 1993 | 148359.31 | 389.73 | 2387.65 | 2553.63 | 54.54 | 74.37 |
| 1994 | 265261.53 | 686.57 | 4270.66 | 4567.56 | 98.18 | 132.99 |
| 1995 | 402606.20 | 1055.81 | 6479.64 | 6930.10 | 148.11 | 201.80 |
| 1996 | 572748.20 | 1501.86 | 9218.07 | 9858.91 | 210.86 | 287.43 |
| 1997 | 666825.50 | 1740.00 | 10733.09 | 11479.24 | 245.64 | 333.86 |
| 1998 | 700447.54 | 1847.20 | 11270.07 | 12053.54 | 256.44 | 350.45 |
| 1999 | 1074156.20 | 2809.71 | 15355.29 | 16422.74 | 394.62 | 536.85 |
| 2000 | 1600960.40 | 4237.68 | 17618.53 | 18843.39 | 584.48 | 799.68 |
| 2001 | 2168291.80 | 5759.80 | 23899.53 | 25560.94 | 790.67 | 1083.21 |
| 2002 | 1556745.44 | 4128.80 | 17143.31 | 18335.13 | 568.46 | 778.24 |
| 2003 | 1020624.26 | 2706.52 | 11238.36 | 12019.63 | 372.74 | 510.21 |
| 2004 | 1679552.00 | 1579.14 | 8293.16 | 8869.69 | 308.16 | 838.79 |
| 2005 | 1966986.08 | 1846.31 | 9710.31 | 10385.36 | 360.39 | 981.59 |
| 2006 | 4317069.60 | 4065.92 | 21321.10 | 22803.32 | 793.17 | 2157.03 |
| 2007 | 5463122.00 | 5149.61 | 26984.33 | 28860.24 | 1004.47 | 2731.09 |
| 2008 | 8709783.94 | 1683.65 | 23056.82 | 30179.03 | 328.54 | 4358.90 |
| 2009 | 2607316.40 | 508.39 | 6914.34 | 9050.18 | 99.09 | 1315.71 |
| 2010 | 4503642.00 | 877.18 | 11943.10 | 15632.38 | 170.98 | 2270.63 |
| 2011 | 3926187.00 | 4344.27 | 4651.15 | 7830.22 | 273.60 | 1985.83 |
| 2012 | 5107612.00 | 8149.89 | 5374.35 | 9047.73 | 206.35 | 2612.80 |
| 2013 | 10698583.00 | 17778.79 | 10860.09 | 18283.00 | 395.10 | 5478.38 |
| 2014 | 11606514.00 | 20143.02 | 9349.15 | 15739.26 | 292.13 | 5952.42 |
| 2015 | 14632346.00 | 12160.33 | 12087.24 | 20348.92 | 401.62 | 8408.63 |
| 2016 | 17734481.00 | 14924.17 | 14750.89 | 24833.16 | 484.54 | 10185.56 |
| 2017 | 15125665.00 | 12218.61 | 12174.52 | 20495.75 | 404.98 | 8702.10 |
| 2018 | 14874038.00 | 9122.06 | 7905.71 | 13309.31 | 332.43 | 8883.38 |
| 2019 | 13449186.00 | 8367.86 | 7107.59 | 11965.64 | 293.24 | 8292.47 |
| 2020 | 14300697.00 | 8898.39 | 7558.46 | 12724.69 | 311.84 | 8817.56 |
| 2021 | 13271720.00 | 8258.85 | 7015.49 | 11810.59 | 289.45 | 8183.14 |

Table S4. MOVES3 Emission Output for Glider Kit Vehicles.

| Emissions in grams/day | | | | | | |
|---|---|---|---|---|---|---|
| Type 49 (Glider Kit Trucks) | | | | | | |
| Chassis MY | Atmospheric CO2 | CO | NO as NO2 | NOx | Total HC | VMT |
| 2009 | 23761.63 | 65.57 | 214.72 | 281.05 | 8.85 | 11.98 |
| 2010 | 28792.57 | 79.43 | 260.17 | 340.53 | 10.72 | 14.51 |
| 2011 | 66303.59 | 182.86 | 465.77 | 784.13 | 24.67 | 33.38 |
| 2012 | 215506.60 | 594.45 | 1513.96 | 2548.76 | 80.20 | 108.54 |
| 2013 | 313811.80 | 865.74 | 2204.64 | 3711.51 | 116.80 | 158.11 |
| 2014 | 424973.60 | 1172.68 | 2985.75 | 5026.51 | 158.22 | 214.23 |
| 2015 | 703837.20 | 2004.80 | 4981.11 | 8385.70 | 273.98 | 387.56 |
| 2016 | 1150590.00 | 3277.34 | 8142.83 | 13708.44 | 447.88 | 633.57 |
| 2017 | 710318.00 | 2023.37 | 5027.06 | 8463.05 | 276.53 | 391.22 |
| 2018 | 1163405.00 | 1449.90 | 8233.68 | 13861.44 | 198.16 | 640.79 |
| 2019 | 476374.90 | 599.15 | 3377.62 | 5686.23 | 82.56 | 270.96 |
| 2020 | 476311.80 | 599.07 | 3377.19 | 5685.50 | 82.54 | 270.93 |
| 2021 | 446479.60 | 561.54 | 3165.66 | 5329.40 | 77.37 | 253.95 |

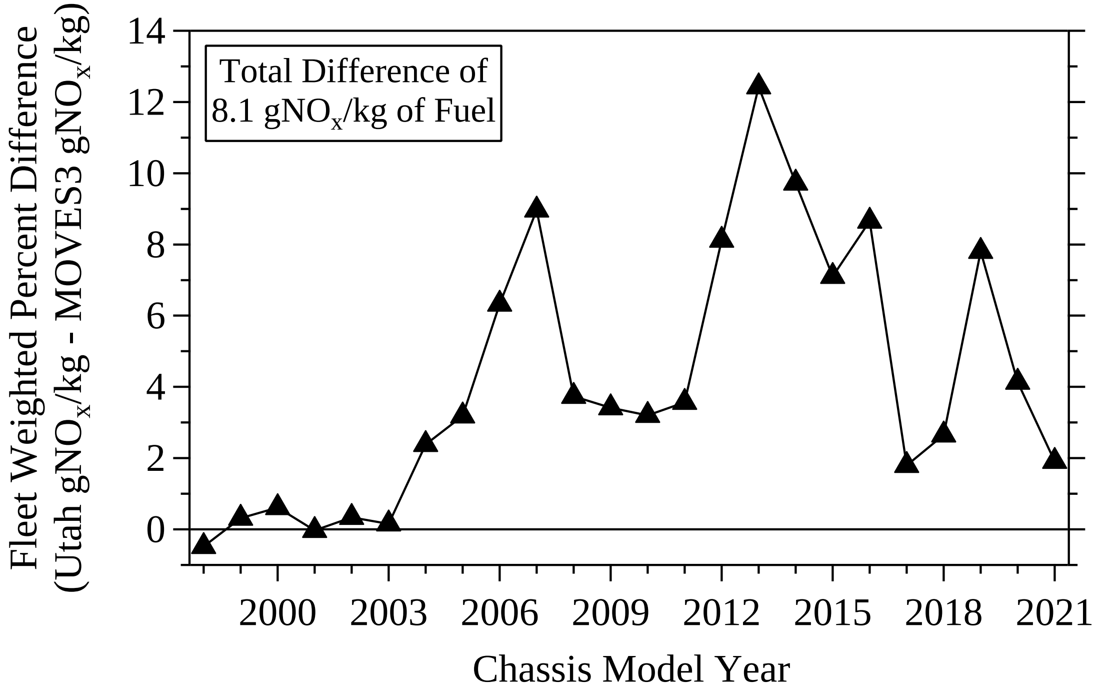


**Figure S13.** Percent difference in the Utah fleet weighted Utah $NO_x$ emission factors minus the Utah fleet weighted MOVES3 $NO_x$ emission factors versus chassis model year. Chassis model year 1998 is a composite of 1998 and older chassis model years. Total difference in the means is 8.1 $gNO_x$/kg of fuel.

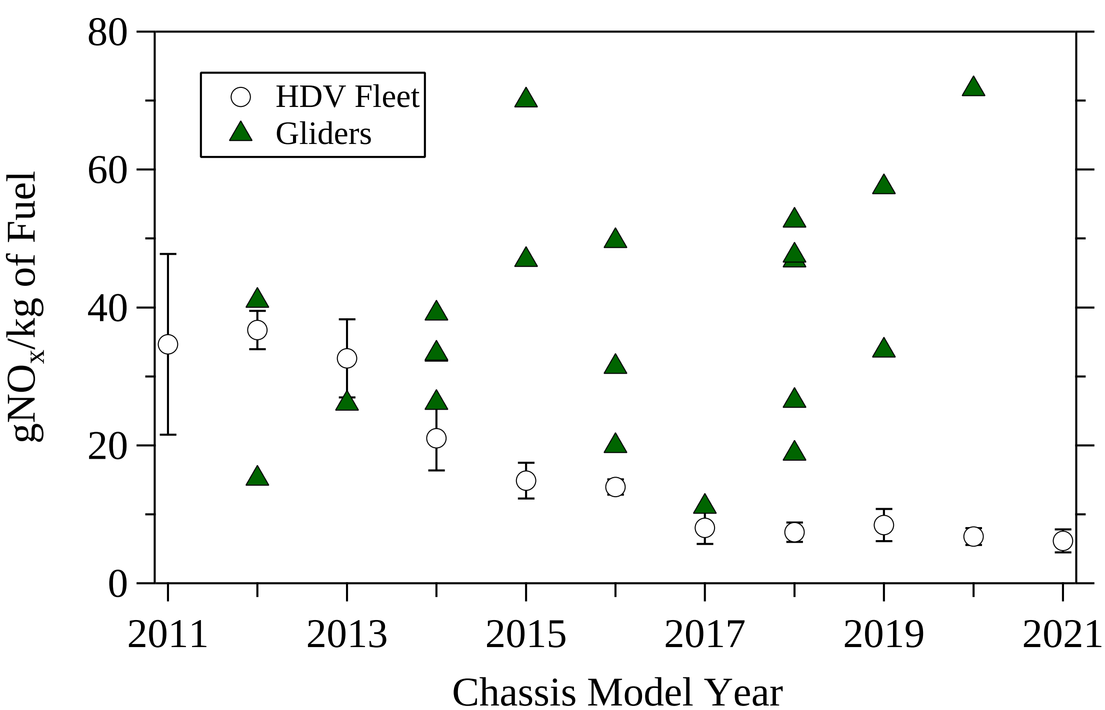


**Figure S14.** Fuel specific $NO_x$ emissions versus chassis model year for chassis model years 2011 and newer compared to individual $NO_x$ emissions from HDV identified as Gliders. Uncertainties are standard error of the mean calculated using the daily means.

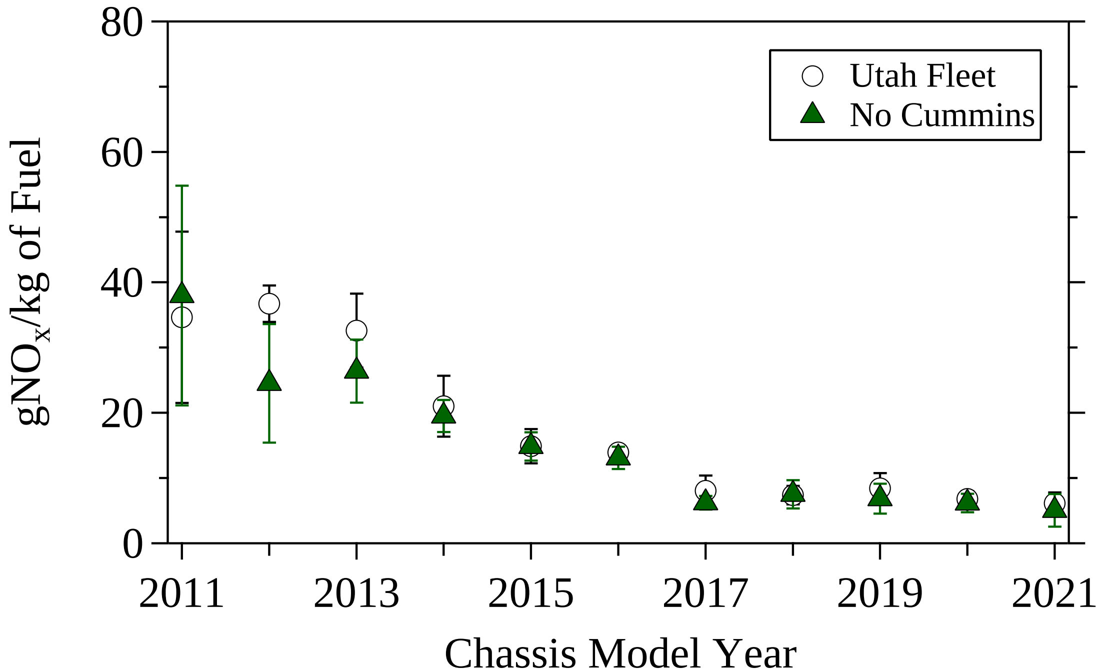


**Figure S15.** Utah fleet fuel specific $NO_x$ emissions versus chassis model year for chassis model years 2011 and newer compared against that same fleet minus all the HDV powered by Cummins engines. Uncertainties are standard error of the mean calculated using the daily means.

Literature Cited

1. Stanton, D., Systematic Development of Highly Efficient and Clean Engines to Meet Future Commercial Vehicle Greenhouse Gas Regulations. *SAE Int. J. Engines* **2013,** 6, 1395-1480, DOI: 10.4271/2013-01-2421.
2. FEAT Math II. Bishop, G. A. https://digitalcommons.du.edu/feat_publications/111/.